DIPLOMARBEIT

Titel der Diplomarbeit

„Local Cluster Expansion for the Treatment of Vacancy Energies in Ni_3Al“

Verfasserin

Barbara Knöbl

angestrebter akademischer Grad

Magistra der Naturwissenschaften (Mag.rer.nat.)

Wien, 2012

Studienkennzahl lt. Studienblatt:	A 411
Studienrichtung lt. Studienblatt:	Diplomstudium Physik UniStG
Betreuerin / Betreuer:	Ao. Univ.-Prof. Dr. Wolfgang Püschl

Danksagung

Ich möchte mich an dieser Stelle bei all den Personen bedanken, die mich bei der Erstellung dieser Arbeit unterstützt haben.

Ein besonderer Dank gilt meinem Betreuer Ao.Univ.-Prof. Dr. Wolfgang Püschl, der mir ein interessantes und anspruchsvolles Thema vorgeschlagen hat und mich mit viel Engagement und guten Ideen betreut hat. Insbesondere danke ich ihm, dass er stets für mich ansprechbar war und mir die Freiheit gelassen hat, die Arbeit nach eigenen Vorstellungen zu entwickeln.

Außerdem möchte ich mich herzlich bei Dr. Martin Leitner bedanken, der mir die in der Arbeit verwendeten DFT-Rechnungen zur Verfügung gestellt hat. Weiters danke ich ihm für etliche hilfreiche Diskussionen, nicht nur zur Implementierung der Probleme.

Nicht zuletzt gilt mein besonderer Dank meinen Eltern, die mir mein Studium ermöglicht haben und mich nicht nur finanziell sondern auch moralisch unterstützt haben.

Abstract

Many properties of solids depend on atomic migration behavior, which is nowadays very often studied by the Monte Carlo simulation technique. For each atom jump it involves the calculation of ΔE, the energy difference between the initial and the final state of the system. Hence the accuracy of any Monte Carlo calculation relies on the accurate knowledge of the *energy* of the respective atomic arrangements which is usually calculated by (semi-) heuristic models or Density Functional Theory (DFT) methods. The latter are in principle exact but require a large computational effort, therefore their application is limited to relatively simple systems (highly ordered structures of only few constituents). The Cluster Expansion (CE) is a mathematically exact method by which the accuracy of DFT calculations can in principle be transferred to much larger calculation cells. For binary alloy systems it is today a well-proven expansion of the possibilities offered by DFT

The CE of the energy $E = E(\sigma)$ of an intermetallic is a series expansion

$$E(\sigma) = \sum_i V_i \Phi_i(\sigma)$$

into effective cluster interactions (ECI) V_i on geometric figures i on the underlying Bravais lattice and their related cluster functions Φ_i , which are relatively simple functions on the lattice occupation. The CE mathematically amounts to a switch from a basis in real space coordinates to a basis in configuration space. Since the exact analytic expression for the internal energy of quantum mechanical systems is usually not known this basis switch is performed by fitting the set of ECIs to a set of known configurations' energies, e.g. DFT calculations (Connolly-Williams method).

If atomic migration takes place by a vacancy mechanism then the vacancy (V) must be introduced as a third atomic. The treatment via DFT is then even more computationally expensive. The CE can in principle capture multicomponent systems, but the procedure is by far more complicated and the fitting of the ECI requires a very large input set. Since their concentration is very low in real metals vacancies can be treated as local disturbances. This can be done by the Local Cluster Expansion (LCE).

We calculated an LCE for the technologically interesting Ni-Al-system. The input set for the fit consisted of defect configurations of the stoichiometric composition of $L1_2$ and $D0_{22}$ $\mathrm{Ni_3Al}$, thus its validity is limited to a narrow concentration range.

Zusammenfassung

Viele Eigenschaften kristalliner Festkörper werden von Diffusion im Festkörper bestimmt. Die Bewegung einzelner Atome durch den Kristall wird häufig mittels Monte-Carlo Simulationen untersucht. Dabei muss für jeden möglichen Atomsprung die Energiedifferenz ΔE zwischen Ausgangs- und Endzustand des Kristalls bekannt sein. Die Genauigkeit der Monte-Carlo Simulationen hängt also von der genauen Kenntnis der potentiellen Energie der betreffenden Struktur ab, welche mittels Dichtefunktionaltheorie (DFT) oder heuristischer Modelle berechnet werden kann. DFT Rechnungen sind grundsätzlich exakt, benötigen aber einen hohen Rechenaufwand und sind daher auf verhältnismäßig einfache Systeme beschränkt, wie beispielsweise hoch geordnete Strukturen aus wenigen Atomsorten. Die Cluster-Entwicklung (CE) ist eine mathematisch exakte Methode, mit der die Genauigkeit der DFT Rechnungen auf weit größere Rechenzellen übertragen werden kann. Gerade für binäre Legierungssysteme ist sie heute eine Standardmethode. Die CE der potentiellen Energie ist eine Reihenentwicklung

$$E(\sigma) = \sum_i V_i \Phi_i(\sigma)$$

in Clusterfunktionen $\Phi_i(\sigma)$ auf geometrischen Figuren (Clustern) am Gitter und in effektive Clusterwechselwirkungen V_i. Vom Standpunkt der Linearen Algebra ist die CE ein Basiswechsel von den kartesischen Koordinaten am Gitter in den Konfigurationsraum. Da es im Allgemeinen aber keinen analytischen Ausdruck für die Funktion $E(\sigma)$ gibt, können die Entwicklungskoeffizienten, die V_i, nicht direkt berechnet werden und müssen mittels Fit an eine Menge bereits bekannter Energien ermittelt werden (Connolly-Williams Methode).

Für die Beschreibung des Leerstellenmechanismus der Diffusion muss die Leerstelle grundsätzlich als dritte Atomsorte behandelt werden. Die CE ist zwar auf Systeme mit beliebig vielen Atomsorten anwendbar, die Beschreibung wird aber sehr aufwendig. Im Falle der verdünnten Leerstellenkonzentration kann die Ternäre CE aber umgangen werden, indem man die Leerstellen als lokale Störungen im Kristall mittels der Lokalen Cluster-Entwicklung (LCE) behandelt.

Wir haben eine LCE für die technologisch interessante Superlegierung Ni_3Al berechnet. Dabei haben wir an $L1_2$ und $D0_{22}$ Defekt-Konfigurationen gefittet. Die Gültigkeit der LCE ist daher auf diesen Konzentrationsbereich beschränkt.

Contents

1 Introduction 11

1.1 Modeling Atomic Migration 11
1.2 The Problem of the Calculation of the Configurational Energy 12
1.3 Cluster Expansion 13
1.4 A Note on Language Use 14

2 The Theoretical Concepts of Cluster Expansion Methods 15

2.1 Configuration space 15
2.2 Connolly Williams Direct Inversion Method 17
2.3 Mathematical Fundamentals of the Cluster Expansion 21
2.4 CE on Periodic Structures: Classes of Clusters 25
2.5 The Objective of the CE: The Use of the CE as Alternative to DFT 29
2.6 Convergence 30
  2.6.1 Heuristic Hints for the Convergence of the CE 31
  2.6.2 The CE of the electrostatic Madelung energy 32
2.7 Truncation 34
  2.7.1 An Hierarchical Approach to Cluster Selection 34
  2.7.2 Using a Genetic Algorithm for Cluster Selection 35
2.8 Calculating the ECIs 37
2.9 Relaxations 38
2.10 Coherent Superlattices 39
2.11 Mixed Space CE 40
2.12 The Treatment of Vacancies in Solids: The Local Cluster Expansion 41

3 Documentation of the Computational Methods 45

3.1 Preparations 45
  3.1.1 Configurations 45
  3.1.2 Clusters 46
3.2 Calculation of the LCE Correlations 49

3.3 Calculation of the LECI 50
3.4 Some Details on the Computational Procedure of the Binary CE 52
3.4.1 The calculation of the Cluster Functions 52
3.4.2 Further Procedure 53
3.5 Cross Validation 53

4 Results, Discussion and Outlook 55

A Supplements to the LCE Results and Documentation 65

B Curriculum Vitae 71

Chapter 1

Introduction

1.1 Modeling Atomic Migration

For many technical applications it is desirable to be able to predict the bulk properties and dynamics of alloy crystals. The dynamic behavior of a multicomponent system is of particular interest, such as atomic migration (diffusion), phase transitions or movements of dislocations. The latter governs mechanical properties of crystals, such as hardening in bulk alloys [1]. Atomic migration (diffusion) can be seen as the basic mechanism of dynamic behavior. The vacancy mechanism, where an atom moves to an unoccupied lattice site and thus 'changes sites with a vacancy', is of outstanding importance, as all crystals exhibit a non-vanishing vacancy concentration at finite temperatures [2, 3], not to speak of structural vacancies [2]. The theoretical treatment of atomic migration is comprehensively described in Refs. [2–4].

We are particularly interested in the vacancy diffusion in Ni-Al alloys, especially the 'superalloy' $\mathrm{Ni_3Al}$ fcc phase which has technologically desirable properties.

The modeling of atomic dynamics and of temperature dependent properties can be performed by Kinetic Monte Carlo (MC) simulations. An overview of the MC technique and other simulation methods is given in [5]. MC simulations involve the evaluation of

$$P(\text{atom jump}) \propto \exp\left[-\frac{\Delta U(\sigma)}{k_B T}\right] \tag{1.1}$$

where P is the probability of one single atomic jump, k_B is the Boltzmann constant, T is the temperature and ΔU is the energy difference between the state of the crystal before and after the atomic jump in question. Thus it is crucial to know the *potential energy of the current atomic arrangement* σ in every single MC step.

1.2 The Problem of the Calculation of the Configurational Energy

The Schrödinger equation

$$\hat{H}\Psi = E\Psi \tag{1.2}$$

contains in principle all information about the atomic system and particularly the ground state potential energy. The definition of its constituents, however, is a delicate task for many-body systems. The Schrödinger equation for the solid state system is formulated in the Born-Oppenheimer approximation: Due to the large mass difference of the electrons and the nuclei the time scales of their movements differ by magnitudes and hence their kinetics can be treated independently. Additionally only electrostatic potentials are considered. The electronic Schrödinger equation of the system of atoms of one species, each with charge Ze, at positions $\mathbf{R}$ and with N electrons i of mass e at positions $\mathbf{r_i}$ is thus

$$\hat{H}\Psi_{el} = \sum_{i=1}^{N}\left(-\frac{\hbar^2}{2m}\nabla_i^2\Psi_{el} - Ze^2\sum_{\mathbf{R}}\frac{1}{|\mathbf{r_i}-\mathbf{R}|}\Psi_{el}\right)+\frac{1}{2}\sum_{i\neq j}\frac{e^2}{|\mathbf{r_i}-\mathbf{r_j}|}\Psi_{el} = E\Psi_{el} \tag{1.3}$$

where Ψ_{el} is the electronic wave-function, in the simplest case a function of the $\mathbf{r_i}$ and the quantum-mechanical spins. Hence the Schrödinger equation of the many-body system Eqn. 1.3 implicitly contains quantum-mechanical effects, although $\hat{H}$ is a quasi-classical operator. For more details on the description of the quantum mechanics of the solid we refer to the textbook by Ashcroft and Mermin [6].

In the general case the many-body-Schrödinger equation cannot be solved analytically, as it is a highly coupled partial differential equation. It was proved by Hohenberg and Kohn [7] that the ground state energy E_0 of an atomic system is uniquely related to its ground state electron density ϱ_0 and is therefore a functional $E_0[\varrho_0]$ of the ground state electron density. Eqn. 1.3 can then be simplified to an effective Schrödinger equation of one particle (*Kohn-Sham equation* [8]). This method to calculate the potential energy from first principles (*ab initio*) is called the *Density Functional Theory* (DFT). Since DFT evaluates the electronic Schrödinger equation 1.3 it is often referred to as 'electronic structure calculations'. A comprehensive description of DFT itself and the computational concept of DFT calculations can be found in [6] or [9].

The effective application of DFT relies on the performance of potent computer systems. It is however still limited to relatively small systems up to some hundreds of atoms per calculation supercell, which means DFT is effectively restricted to highly symmetric ordered crystalline structures. It is in principle possible to study defects, interfaces and surfaces, layered systems and even disorder by DFT, but its application to these problems or even to short-range order (SRO) is limited. Due to its high computational cost its direct application in MC simulations (*ab initio MC*) is only feasible for relatively simple systems and few MC steps.

There are many approximative methods for the calculation of the potential energy of many-body systems, the most common involve pairwise interactions, e.g. Lennard-Jones-Potentials and mean field approximations, e.g. embedded atom method (EAM), which often need to be adjusted to experimental findings. [5, 6, 10]

1.3 Cluster Expansion

Still it would be desirable to make simulations and other predictions under as few assumptions as possible. The Cluster Expansion (CE) method of Sanchez, Ducastelle and Gratias [11] promises *ab initio* accuracy at a low computational cost. To that end, the energy $E(\sigma)$ is examined on a fixed Bravais lattice L. The lattice is occupied with a certain number m of atomic species, each distinct occupation is called a *configuration*. The idea of the CE [11] is to switch the basis from real space coordinates to the *configuration space*. This means that the function $E(\sigma)$ is expanded in terms of so-called cluster functions $\Phi_i(\sigma)$

$$E(\sigma) = \sum_i V_i \Phi_i(\sigma) \tag{1.4}$$

Once the V_i are known, the function of the energy is a sum of easily calculable terms: The cluster functions are simple functions of the lattice occupation, e.g. spin products or correlation functions (cf. section 2.3); the coefficients V_i, the *effective cluster interactions* (ECIs), themselves are scalars. Eqn. 1.4 is particularly simple for binary alloys, as we will discuss later in this work. Hence the CE can be used to calculate the configurational energy of the current atomic arrangement in each MC step to gain temperature dependent thermodynamic potentials and the atomic dynamics in general. The challenge of CE calculations is to find the values of the values of the V_i.

For the use of the CE in atomic migration model calculations it is in principle necessary to treat the vacancy as an atomic species of its own, and hence the study of vacancy diffusion in binary alloys involves a ternary CE [12]. The ternary CE, though, is by far more sophisticated compared to the binary CE. For dilute vacancy concentrations, where there is no vacancy-vacancy interaction, however, the energy of the crystal can be described through a Local Cluster Expansion (LCE) [4, 13–15], which is, very roughly described, a modified binary CE.

The main application of the CE, though, has been the calculation of phase diagrams. The CE may in principle search *all* possible configurations σ, at least up to a certain size of the crystallographic unit cell. Calculating the $T = 0K$ phase diagram by means of DFT involves the calculation of the energies of some (possibly several dozens) suitably chosen configurations of the alloy system (*'usual suspects'*). The convex hull of the respective formation enthalpies is then the ground state line. This method is likely to miss the real physical ground state, if it was not *coincidentally* in this set. This is particularly the case for low energy ground states which are unstable at room temperature, e.g. in the Cu-Zn alloy system (brass) [16], where there is hence little experimental evidence for their existence. Similar was observed in calculations for the bcc Ta-W system [17].

The evaluation of the CE is a delicate task, hence there are many projects for minimum-user-input-programs, e.g. the Alloy Theoretic Automated Toolkit (ATAT [18]). The Universal Cluster Expansion (UNCLE [19]) is the most promising among them, although presently not yet available for general usage.

The cluster expansion is based on the Cluster Variation Method (CVM) of Kikuchi [20] in thermodynamics, the first major publications were Refs. [21] in 1979 and [22] in 1981. The Connolly-Williams-method [23], which is described later in this work, was presented in 1983. The fundamental mathematical description, a mathematical formulation independent of the preceding work, though, was given in 1984 by Sanchez, Ducastelle and Gratias [11]. This work has become the standard reference on CE. Valuable reviews of the CE method include Refs. [16, 19, 24–27].

1.4 A Note on Language Use

In principle the terms 'alloy' and 'intermetallic' (or 'intermetallic compound') do not stand for the same solid state phases. Roughly spoken, while 'alloy' is often used for crystalline mixtures of metals, possibly with nonmetallic constituents, with no particular order, 'intermetallic' refers to ordered compounds of metallic and possibly nonmetallic constituents. A comprehensive description is given in Ref. [28]. In the field of cluster expansion this distinction is usually omitted, since it is clear that the study focuses on monocrystalline structures of a number of constituents, i.e. configurations on an underlying Bravais lattice, which are often called *substitutional alloys*. Therefore we use these terms synonymously, too.

Chapter 2

The Theoretical Concepts of Cluster Expansion Methods

2.1 Configuration space

Let L be a Bravais lattice, a set of N atomic positions p_i (or simply p) with translational symmetry. We restrict the discussion to lattice parameter $a = 1$, without loss of generality. We can define a certain crystalline structure by assigning an atom of any of m (elemental) constituents to each lattice site p_i. A distinct distribution of the crystal's constituents onto the lattice sites p_i is called a configuration on the lattice.

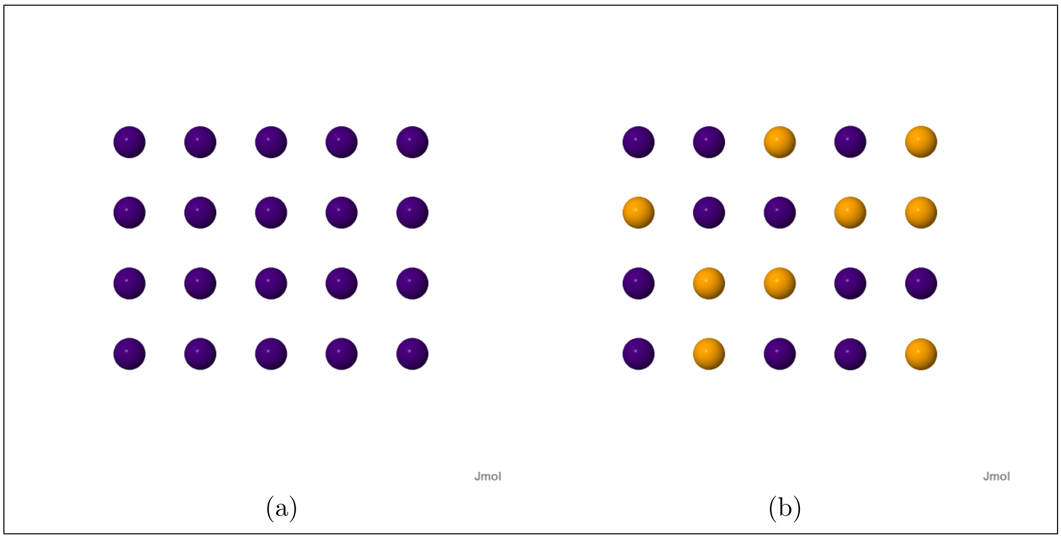

(a) (b)

Figure 2.1: Configurations on a two-dimensional lattice. (a) A two-dimensional lattice; (b) a random configuration of two species;

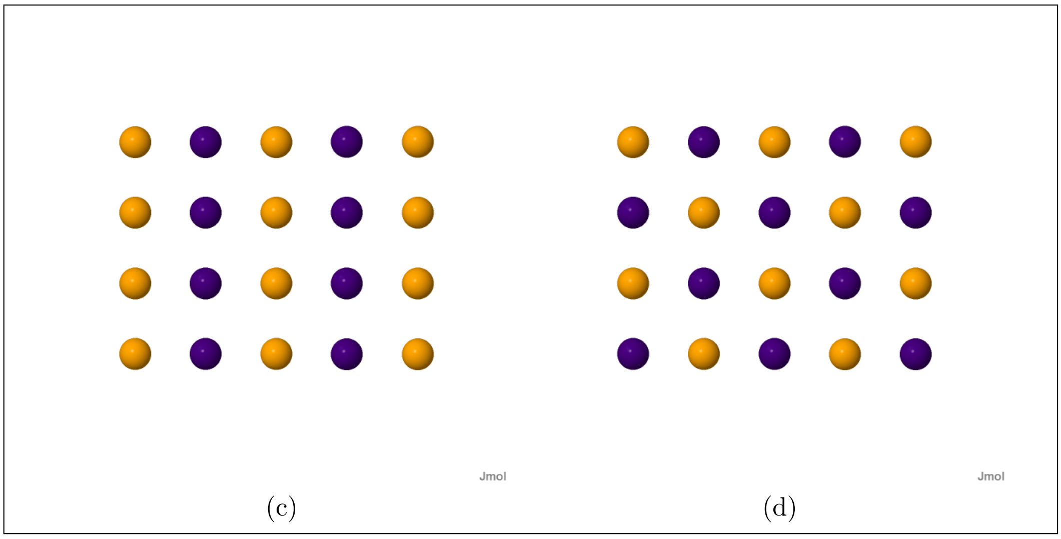

(c) (d)

Figure 2.1: (c), (d) two ordered configurations.

With the lattice type fixed, we can then describe the crystal by a *configuration vector* σ where each vector component i refers to a lattice vector p_i. We assign a certain occupation variable σ to each constituent. The entries σ_i of the configuration vector are the occupation variables, depending on which constituent is occupying site i.

$$\sigma = (\sigma_{p_1}, \sigma_{p_2}, ..., \sigma_{p_N}) \tag{2.1}$$

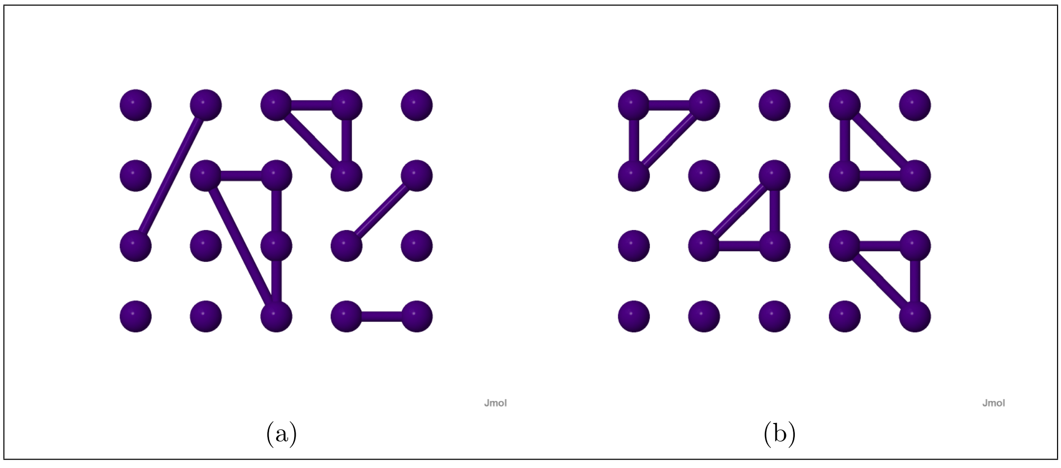

(a) (b)

Figure 2.2: (a) Clusters in a two-dimensional lattice, (b) symmetric triangles.

For binary crystals we can define

$$\sigma_{p_i} = \begin{cases} +1, & \text{if } p_i \text{ occupied by A atom} \\ -1, & \text{if } p_i \text{ occupied by B atom} \end{cases} \quad .$$

These particular occupation variables are often called *spin variables.* The set of all possible configuration vectors forms the configuration space [16, 24–27]. If the number of sites in L is N it is clear that the number of possible configurations is m^N.

Before we concentrate on functions of the configuration we introduce some additional terms on the lattice. Let α be a set of k lattice sites in L,

$$\alpha = \{p_{i_1}, p_{i_2}, p_{i_3}, ..., p_{i_k}\} \tag{2.2}$$

for instance an arbitrary set of three nearest neighbors in an fcc lattice (a *nearest-neighbor triangle*). These geometrical subsets are called the **clusters** and their cardinality k is called the *order* of the cluster. In a lattice of N atomic sites there are 2^N distinct clusters.

Obviously there are many congruent clusters in Bravais lattices. These are related by the operations $\hat{R}$ of the lattice's space group. The explicit representation of the symmetry operations in each space group is not uniquely defined, as reflections can be represented by a rotation followed by the inversion, but its cardinality is, indeed, a unique number. The set of all symmetry related clusters is denoted f_α or simply f. Hence the term *cluster* refers both to the distinct cluster α and to the set f of symmetric clusters.

2.2 Connolly Williams Direct Inversion Method

We start with an introductory example to illustrate the mathematical concept of the CE, presenting the Direct Inversion Method of Connolly and Williams [23], an early application of the CE to binary alloys.

Let σ_n be one particular ordered atomic arrangement of atoms of kind A and B on an fcc lattice. Figure 2.3 shows some highly ordered fcc configurations.

We have introduced the spin operator $\sigma(p_i)$ on the binary lattice before. Hence we have

$$\sigma = (\sigma_{p_1}, \sigma_{p_2}, ..., \sigma_{p_N}) \quad .$$

In the simple case of a binary configuration, the cluster functions are the multisite correlation functions which are averages of spin products

$$\xi_f = \frac{1}{N_f} \sum_f \sigma_{p=\alpha_1} \sigma_{p=\alpha_2} ... \sigma_{p=\alpha_k} \tag{2.3}$$

where α_i denote the edges $p_1, p_2, ..., p_k$ of one particular k-point cluster α . The sum runs over all clusters α of type f in the lattice and N_f is their total

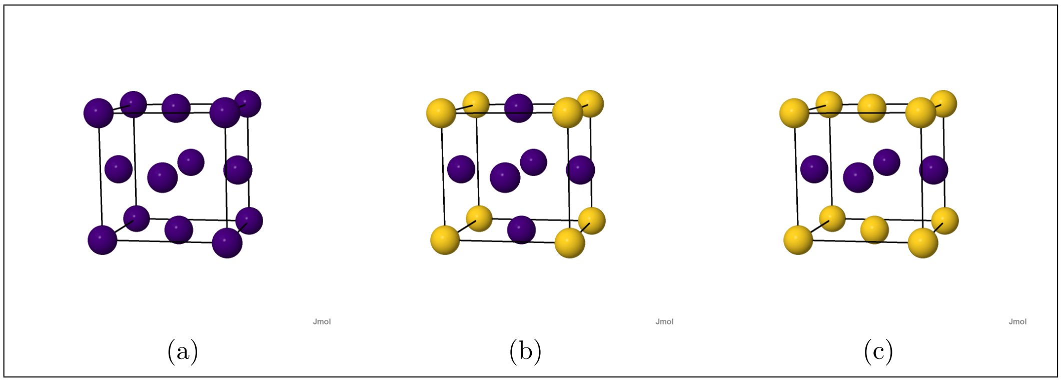

(a) (b) (c)

Figure 2.3: Some highly symmetric fcc configurations.(a) pure metal, (b) $L1_2$, (c) $L1_0$. Note that the NN tetrahedron is a basis cell for each.

number. For example, for nearest-neighbor(NN) triangles in an $L1_2$ lattice it holds that

$$\xi_{\text{NN triangle}} = \frac{1}{4}[(-1)(-1)\cdot 1+(-1)(-1)\cdot 1+(-1)(-1)\cdot 1+(-1)(-1)(-1)] = \frac{1}{2}$$

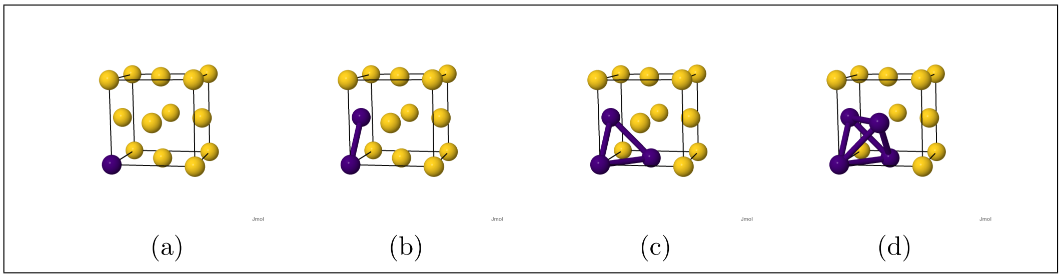

(a) (b) (c) (d)

Figure 2.4: Clusters of the NN-tetrahedron approximation: Null cluster (no picture), point (a), NN-pair (b), NN-triangle (c), NN-tetrahedron(d).

We note that it is sufficient to evaluate the four triangles in the tetrahedron, because the $L1_2$ crystal consists merely of such tetrahedrons, cf. Figure 2.3. Counting all tetrahedra would obviously just expand the fraction.

Connolly and Williams [23] investigated phase transformations of 4d-transition-metal binary alloys and therefore used the CE to calculate the formation enthalpies of the disordered states. For the binary random solid solution it can be shown that [23]

$$\xi_k = (x_A - x_B)^k \tag{2.4}$$

with the relative concentrations x_A, x_B of A and B atoms, respectively. Together with the effective interactions, V_k, the internal energy E_D if the dis-

Table 2.1: Correlations of the input set

	ξ_0	ξ_{point}	ξ_{pair}	$\xi_{triplet}$	$\xi_{tetrah.}$
A	1	1	1	1	1
A_3B	1	$\frac{1}{2}$	0	$-\frac{1}{2}$	-1
AB	1	0	$-\frac{1}{3}$	0	1
AB_3	1	$-\frac{1}{2}$	0	$\frac{1}{2}$	-1
B	1	-1	1	-1	1
$\sigma_A = 1$, $\sigma_B = -1$					

ordered state is

$$E_D = \sum_k V_k (x_A - x_B)^k \quad . \tag{2.5}$$

To calculate a set of effective interactions V_k, Connolly and Williams [23] chose four clusters – point, NN pair, NN triangle, NN tetrahedron – and five basic fcc structures, pure A (fcc), A_3B ($L1_2$), AB ($L1_0$), AB_3 ($L1_2$), pure B (fcc). These structures make up the so-called input set. The internal energies $E_n(r)$ of the input set of 4d-transition-metal binary alloys were calculated via first-principles methods [23]. The corresponding correlation functions, including the null-cluster ($\xi_0 = 1$ for all σ_n), are listed in table 2.1. Hence we obtain a set of equations with variables V_k, in matrix notation

$$\begin{pmatrix} E_A(r) \\ E_{A_3B}(r) \\ E_{AB}(r) \\ E_{AB_3}(r) \\ E_B(r) \end{pmatrix} = \begin{pmatrix} 1 & 1 & 1 & 1 & 1 \\ 1 & \frac{1}{2} & 0 & -\frac{1}{2} & -1 \\ 1 & 0 & -\frac{1}{3} & 0 & 1 \\ 1 & -\frac{1}{2} & 0 & \frac{1}{2} & -1 \\ 1 & -1 & 1 & -1 & 1 \end{pmatrix} \begin{pmatrix} V_0(r) \\ V_1(r) \\ V_2(r) \\ V_3(r) \\ V_4(r) \end{pmatrix} \quad . \tag{2.6}$$

We note that the energy depending on r, the lattice parameter, is used here, in contrast to the energy of the fully relaxed structure as equation 1.4 in the introduction implies, thus leading to r-dependent $V_k(r)$. It is indeed the case that the use of an unrelaxed input set yields unrelaxed $V_k(r)$ while fully relaxed input sets lead to fully relaxed V_k [26]. In order to calculate $E_n(r)$ of one configuration several DFT calculations for different lattice parameters are performed, and the values $E_n(r)$ (of one configuration n) are fitted to a Lennard-Jones-type potential [29].

Obviously, calculating the $V_k(r)$ simply requires inversion of the matrix,

$$\begin{pmatrix} V_0(r) \\ V_1(r) \\ V_2(r) \\ V_3(r) \\ V_4(r) \end{pmatrix} = \begin{pmatrix} 1 & 1 & 1 & 1 & 1 \\ 1 & \frac{1}{2} & 0 & -\frac{1}{2} & -1 \\ 1 & 0 & -\frac{1}{3} & 0 & 1 \\ 1 & -\frac{1}{2} & 0 & \frac{1}{2} & -1 \\ 1 & -1 & 1 & -1 & 1 \end{pmatrix}^{-1} \begin{pmatrix} E_A(r) \\ E_{A_3B}(r) \\ E_{AB}(r) \\ E_{AB_3}(r) \\ E_B(r) \end{pmatrix} . \tag{2.7}$$

We note that for the particular sets of input configurations and clusters chosen the matrix is indeed non-singular and hence invertible.

What we have just described is the Direct Inversion Method for calculating the effective interactions $V_k(r)$, using a given set of energies $E_n(r)$ and the same number of correlation functions ξ_k. The knowledge of the effective interaction energies, V_k, allows to calculate the internal energies $E_{n,D}(r)$ of the disordered states.

This model, however, fails to describe many configurations correctly, such as $L1_1$ or $D0_{22,23}$ whose basis vectors in the crystallographic unit cell themselves are even larger than the clusters adopted within this model. The vector of the correlation functions must uniquely describe one configuration either used as input or for prediction. This condition is more likely to be violated the smaller the cluster set is.

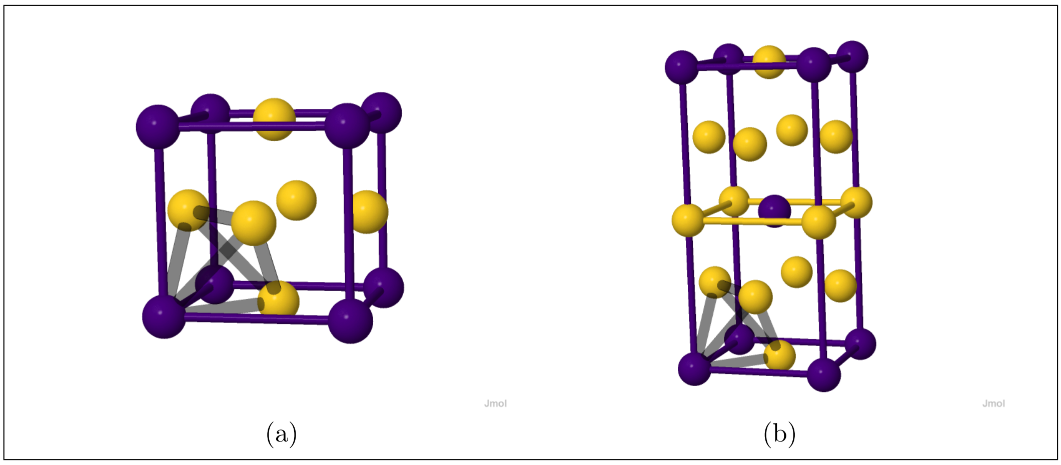

(a) (b)

Figure 2.5: (a) $L1_2$, (b) $D0_{22}$ with the NN tetrahedron.

Example ($L1_2$ and $D0_{22}$ in the nearest neighbor tetrahedron approximation)

Both $L1_2$ and $D0_{22}$ consist entirely of NN-tetrahedrons of 1 A atom and 3 B atoms (or v.v.), cf. Figure 2.5, hence they have the same ξ_i within the NN-tetrahedron approximation.

Nevertheless this simplified model is still being applied, e.g. in [27, 29]; the aim of Ref. [29] was indeed to calculate the energy of the random solid solution and not necessarily the calculation of many new configurational energies.

2.3 Mathematical Fundamentals of the Cluster Expansion

Following Ref. [11] we define the scalar product of two functions $f(\sigma)$ and $g(\sigma)$ in the configuration space

$$\langle f(\sigma), g(\sigma)\rangle = \frac{1}{m^N} Tr^{(N)} f(\sigma)g(\sigma) := \frac{1}{m^N}\sum_{\sigma} f(\sigma)g(\sigma) \tag{2.8}$$

where m is the number of constituents of the crystal and N the number of lattice sites. It is indeed well defined, since the functions f, g are discrete real functions of σ. Any function $f(\sigma)$ can then be written w.r.t. an orthonormal basis $\Phi_i(\sigma)$ as

$$f(\sigma) = \sum_{i=1}^{N}\langle f(\sigma), \Phi_i(\sigma)\rangle \Phi_i(\sigma) = \sum_{i=1}^{N} V_i\Phi_i(\sigma) \tag{2.9}$$

From the definition of the scalar product as a configurational average over all σ it follows that the coefficients

$$V_i = \langle f(\sigma), \Phi_i(\sigma)\rangle \tag{2.10}$$

are constants independent of the configuration σ.

In the following we will introduce the cluster functions $\Phi_i(\sigma)$ as a basis for the description of physical functions of the lattice occupation.

The occupation variable or spin σ_p of a lattice site p shall take the values $\{\pm\frac{m}{2}, \ldots, \pm 1\}$ if m, the number of distinct constituents, is an even number or $\{\pm\lfloor\frac{m}{2}\rfloor, \ldots, \pm 1, 0\}$ if m is an odd number, respectively. We note that this is indeed in full alignment with the binary spins we have introduced before: $m = 2$ and thus $\sigma_p = +1, -1$.

Following Ref. [11] we use the m first Chebychev polynomials Θ_n as basis functions on each lattice site p_i,

$$\Theta_{2j}(\sigma_p) = \sum_{k=0}^{j} c_k^{(j)}\sigma_p^{2k} \tag{2.11}$$

$$\Theta_{2j+1}(\sigma_p) = \sum_{k=0}^{j} d_k^{(j)}\sigma_p^{2k+1} \tag{2.12}$$

where the j take values such that the indices n in Θ_n run from 0 to $m-1$. The coefficients $c_k^{(j)}, d_k^{(j)}$ follow from the orthogonality relation:

$$\langle \Theta_n(\sigma_p), \Theta_{n'}(\sigma_p) \rangle = \delta_{n,n'} \tag{2.13}$$

Note that this choice is merely arbitrary. The Chebychev polynomials, however, are applicable to an arbitrary number of constituents, and turn out to imply particularly convenient basis functions for the binary alloy, as the examples illustrate. Furthermore they are the orthogonalized system of the basis set $\{1, \sigma, \sigma^2, \ldots\}$ gained through the Gram-Schmidt process.

Example (Binary alloy)

For binary configurations we have defined before

$$\sigma_p = \begin{cases} +1, & \text{p occupied by A atom} \\ -1, & \text{p occupied by B atom} \end{cases},$$

thus we have two functions Θ_n

$$\begin{aligned} \Theta_0(\sigma_p) &= c_0 \\ \Theta_1(\sigma_p) &= d_0 \sigma_p \quad . \end{aligned}$$

The functions Θ_n are orthogonal:

$$\begin{aligned} \langle \Theta_0(\sigma_p), \Theta_1(\sigma_p) \rangle &= \frac{1}{2^N} \sum_{\sigma} c_0 d_0 \sigma_p = \frac{1}{2^{N-1}} \underbrace{\sum_{\sigma_{p_1}} \cdots \sum_{\sigma_{p_N}}}_{\text{all } \sigma_{p_i} \text{ except } \sigma_p} \frac{1}{2} \sum_{\sigma_p = \pm 1} c_0 d_0 \sigma_p = \\ &= \frac{2^{N-1}}{2^{N-1}} \frac{1}{2} (c_0 d_0 - c_0 d_0) = 0 \end{aligned}$$

From the normalization

$$\begin{aligned} \langle \Theta_0(\sigma_p), \Theta_0(\sigma_p) \rangle &= c_0^2 \frac{1}{2^N} \sum_{\sigma} 1 = c_0^2 = 1 \\ \langle \Theta_1(\sigma_p), \Theta_1(\sigma_p) \rangle &= d_0^2 \frac{1}{2^N} \sum_{\sigma} \sigma_p^2 = d_0^2 \frac{1}{2} \sum_{\sigma_p = \pm 1} \sigma_p^2 = d_0^2 = 1 \end{aligned}$$

follows that

$$\Theta_0(\sigma_p) = 1 \tag{2.14}$$

$$\Theta_1(\sigma_p) = \sigma_p \quad . \tag{2.15}$$

The orthonormality relation Eqn. 2.13 can be generalized to [11]

$$\langle \Theta_n(\sigma_p), \Theta_{n'}(\sigma'_p) \rangle = \delta_{n,n'}\delta_{p,p'} \tag{2.16}$$

for any two lattice sites p, p', and the following completeness relation can be shown [11]:

$$\sum_{n=0}^{m-1} \Theta_n(\sigma)\Theta_n(\sigma') = m\delta_{\sigma,\sigma'} \tag{2.17}$$

Example (Binary alloy)

The functions (Eqn. 2.14)

$$\begin{aligned} \Theta_0(\sigma_p) &= 1 \\ \Theta_1(\sigma_p) &= \sigma_p \end{aligned}$$

obey the completeness relation Eqn. 2.17

$$\begin{aligned} \sum_{n=0}^{1} \Theta_n(\sigma_p)\Theta_n(\sigma_{p'}) &= (1 \cdot 1) + (\sigma_p + \sigma_{p'}) = \\ &= \begin{cases} 1+1=2 & \text{for } \sigma_p = \sigma_{p'} \\ 1+(-1)=0 & \text{for } \sigma_p \neq \sigma_{p'} \end{cases} \end{aligned}$$

With the functions Θ_n on the sites p we can construct a basis set for the configuration space of the lattice L, the *cluster functions* Φ_i, as products of Θ_n. We had the cluster of order k

$$\alpha = \{p_{i_1}, \ldots, p_{i_k}\}$$

before; now we define a set s of k indices

$$s = \{s_{i_1}, \ldots, s_{i_k}\} \quad .$$

The functions

$$\Phi_{\alpha,s}(\sigma) = \Theta_{s_1}(p_{i_1}) \ldots \Theta_{s_k}(p_{i_k}) \tag{2.18}$$

are the cluster functions $\Phi_{\alpha,s}(\sigma)$. We replaced the index i in Φ_i, which we had not specified yet, by the set (α, s). It was shown [11] that the cluster functions $\Phi_{\alpha,s}(\sigma)$ inherit an orthogonality relation

$$\langle \Phi_{\alpha,s}(\sigma), \Phi_{\alpha',s'}(\sigma) \rangle = \delta_{\alpha,\alpha'}\delta_{s,s'} \tag{2.19}$$

and a completeness relation

$$\sum_s \Phi_{\alpha,s}(\sigma)\Phi_{\alpha,s}(\sigma') = m^k \delta_{\sigma,\sigma'} \tag{2.20}$$

due to the orthogonality and completeness of their constituents Θ_n.

Equation 2.9

$$f(\sigma) = \sum_{(\alpha,s)} V_i \Phi_{\alpha,s}(\sigma)$$

is the **cluster expansion** of the function $f(\sigma)$ of the configuration σ.

Example (Binary alloy)

For the binary case with the functions

$$\begin{aligned} \Theta_0(\sigma_p) &= 1 \\ \Theta_1(\sigma_p) &= \sigma_p \end{aligned}$$

we construct the cluster functions $\Phi_{\alpha,s}(\sigma)$:

- Point cluster $\alpha = p_1$

$$\Phi_{\alpha,s}(\sigma) = \begin{cases} \Theta_0(p_1) = 1 \\ \Theta_1(p_1) = \sigma_{p_1} \end{cases}$$

- Pair cluster $\alpha = (p_1, p_2)$

$$\Phi_{\alpha,s}(\sigma) = \begin{cases} \Theta_0(p_1)\cdot \Theta_0(p_2) = 1 \\ \Theta_0(p_1)\cdot \Theta_1(p_2) = \sigma_{p_2} \\ \Theta_1(p_1)\cdot \Theta_0(p_2) = \sigma_{p_1} \\ \Theta_1(p_1)\cdot \Theta_1(p_2) = \sigma_{p_1}\sigma_{p_2} \end{cases}$$

- Triplet cluster $\alpha = (p_1, p_2, p_3)$

$$\Phi_{\alpha,s}(\sigma) = \begin{cases} \Theta_0(p_1)\cdot \Theta_0(p_2)\cdot \Theta_0(p_3) = 1 \\ \Theta_0(p_1)\cdot \Theta_1(p_2)\cdot \Theta_0(p_3) = \sigma_{p_2} \\ \Theta_1(p_1)\cdot \Theta_1(p_2)\cdot \Theta_0(p_3) = \sigma_{p_1}\sigma_{p_2} \\ \Theta_1(p_1)\cdot \Theta_1(p_2)\cdot \Theta_1(p_3) = \sigma_{p_1}\sigma_{p_2}\sigma_{p_3} \\ \text{etc.} \end{cases}$$

Example (continued.)

By rigid construction we gain the same functions $\Phi_{\alpha,s}$ several times. Thus for the case of the binary system the construction rule 2.18 can be reduced to

$$\begin{aligned}\Phi_{\alpha,s}(\sigma) &= \Phi_\alpha(\sigma) = \Theta_1(p_{i_1})\dots\Theta_1(p_{i_k})\\ \Phi_\alpha(\sigma) &= \sigma_{p_{i_1}}\dots\sigma_{p_{i_k}}\\ \Phi_0(\sigma) &= 1 \quad .\end{aligned} \tag{2.21}$$

These are the well known (e.g. [30]) cluster functions for binary systems. We have shown that these can be gained from a general mathematical formalism for the m-component configuration space. The indices i in $\Phi_i(\sigma)$ are the set of all clusters α in the Lattice L.

If $f(\sigma)$ is the energy $E(\sigma)$ of a binary system and $\Phi_{\alpha,s}$ are the binary cluster functions 2.21 the cluster expansion 2.9 is often written as

$$E(\sigma) = V_0 + \sum_p V_{\text{point}}\sigma_p + \sum_{(p,p')} V_{\text{pair}}\sigma_p\sigma_{p'} + \sum_{(p,p',p'')} V_{\text{triplet}}\sigma_p\sigma_{p'}\sigma_{p''} + \dots \tag{2.22}$$

and due to its resemblance to the magnetic Ising Hamiltonian [6] called *generalized Ising Hamiltonian.*

2.4 CE on Periodic Structures: Classes of Clusters

The description of the CE has not used any particular properties of periodic structures so far and is thus not restricted to Bravais lattices but indeed valid for any arbitrary underlying set of atomic sites **R**. Nevertheless the formulation given above can be drastically simplified taking advantage of the symmetry of infinite lattices [11, 24, 26].

We have mentioned before that each geometric cluster α is associated to its class of symmetry-equivalent clusters f_α

$$f_\alpha = \{\alpha' : \alpha' = \hat{R}\alpha \ , \hat{R} \in \text{space group}\} \tag{2.23}$$

according to the N_L symmetry operations $\hat{R}$ of the space group of the underlying Bravais lattice. For the three cubic Bravais lattices the space group

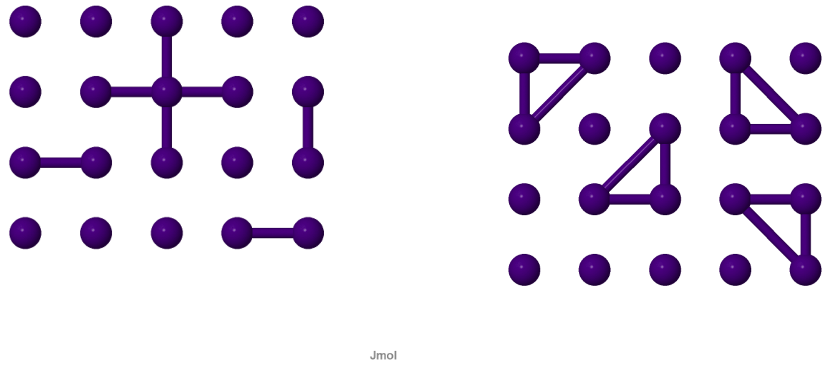

(a) (b)

Figure 2.6: Some symmetric (a) pairs, (b) triangles an a two-dimensional lattice.

consists of the point group O_h of 48 symmetry operations and the translations. It is obvious that N_L is the number of the point group operations on L times the number of sites N. Yet two distinct space group operations might yield congruent $\hat{R}\alpha$, therefore the number of distinct α', ND_{f_α}, is usually smaller. In the following we denote the cluster classes simply as f.

Example (Symmetric clusters in the fcc lattice)

Be L an fcc lattice with $a = 1$. we consider the pair cluster which is one edge of the conventional unit cell,

$$\alpha = \{\vec{0}, (1,0,0)\}$$

(denoted 3-NN pair) and the symmetry operations inversion

$$\hat{R} = \begin{pmatrix} -1 & 0 & 0 \\ 0 & -1 & 0 \\ 0 & 0 & -1 \end{pmatrix}$$

Example (continued.)

and rotation by the z-axis by π

$$\hat{R} = \begin{pmatrix} \cos\pi & -\sin\pi & 0 \\ \sin\pi & \sin\pi & 0 \\ 0 & 0 & 1 \end{pmatrix} = \begin{pmatrix} -1 & 0 & 0 \\ 0 & -1 & 0 \\ 0 & 0 & 1 \end{pmatrix} \quad .$$

These symmtery operations yield the same cluster

$$\alpha' = \{\vec{0}, (-1,0,0)\} \quad ,$$

and the number of inequivalent pair clusters α' is 6.

By counting all distinct clusters α' originating from p which are symmetric w.r.t the point group, for all lattice sites p, we count each cluster k times. Hence, if $D_{f,PG}$ is the number of clusters α' symmetric w.r.t. the point group,

$$D_f = \frac{D_{f,PG}}{k}$$

Some D_f of fcc clusters symmetric w.r.t. to the lattice site $p = (0,0,0)$ are given in table 2.2.

For any crystal property we have [24]

$$g(\hat{R}\sigma) = g(\sigma) \tag{2.24}$$

and it is obvious that

$$\Phi_{\hat{R}\alpha}(\hat{R}\sigma) = \Phi_\alpha(\sigma) \quad . \tag{2.25}$$

Thus it follows for the expansion coefficients (Eqn. 2.10)

$$\begin{aligned} V_{\hat{R}\alpha} &= \langle g(\sigma), \Phi_{\hat{R}\alpha}(\sigma)\rangle \\ &= \langle g(\hat{R}\sigma), \Phi_{\hat{R}\alpha}(\hat{R}\sigma)\rangle \\ &= \langle g(\sigma), \Phi_\alpha(\sigma)\rangle \\ &= V_\alpha \end{aligned} \tag{2.26}$$

since the value of the scalar product $\langle g(\sigma), \Phi_{\hat{R}\alpha}(\sigma)\rangle$ is constant for all σ; in particular it takes the same value for σ and $\hat{R}\sigma$. This means that all symmetry-related clusters α yield the same V_α, which we thus denote V_f. Hence we can factorize V_f and sort the cluster series (Eqn. 2.9) by symmetry-inequivalent terms. We emphasize that we have only used geometric properties of the Bravais lattice, independent of the current configuration σ itself.

Table 2.2: Degeneracies D_{f_α} of some fcc clusters

Cluster type f	D_f	Picture
NN pair	6	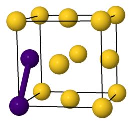
NN triangle	8	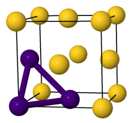
NN tetrahedron	2	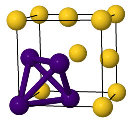

We introduce the 'lattice-averaged cluster functions' [24, 26]

$$\overline{\Pi}_f(\sigma) = \frac{1}{N_L} \sum_{\hat{R}}^{N_L} \Phi_{\hat{R}\alpha}(\sigma) = \frac{1}{ND_f} \sum_{\alpha \in f} \Phi_\alpha(\sigma) \tag{2.27}$$

which are orthogonal [24] and hence we can write

$$g(\sigma) = N \sum_f D_f V_f \overline{\Pi}_f(\sigma) \quad . \tag{2.28}$$

Eqn. 2.28 is particularly useful for the infinite crystal: its properties are usually examined *per atom*, $\tilde{g}(\sigma) = g(\sigma)/N$, and hence the coefficient N in Eqn. 2.28 cancels. The treatment of Eqn. 2.27 for the infinite crystal is described in detail in section 3.4.1.

Example (Binary alloy)

For binary configurations we obtain

$$\overline{\Pi}_f(\sigma) = \frac{1}{ND_f} \sum_{\alpha \in f} \sigma_{p_1} \sigma_{p_2} \dots \sigma_{p_k} \tag{2.29}$$

where p_i are again the vertices of the distinct cluster α. These are the well known multisite correlation functions of a binary crystal. The factor $1/N$ cancels for the infinite crystal: Since there are no effects of alloy-vacuum interfaces, the sum just goes over the point group and the crystallographic basis (i.e. atoms in the unitcell), times N.

2.5 The Objective of the CE: The Use of the CE as Alternative to DFT

Let $f(\sigma)$ be the internal energy $E(\sigma)$. For the sake of simplicity we replace the index set (α, s) or α by consecutive enumeration i. We enumerate starting from 0 to emphasize the null-cluster $\alpha = \{\}$. For the binary case we have 2^N distinct clusters and 2^N distinct configurations σ.

Knowing the set of ECIs $\{V_i\}$, for the function $E(\sigma)$ it is easy to calculate $E(\sigma)$ for any particular σ and hence to plot the phase diagram. The ECIs usually cannot be calculated analytically by evaluating Eqn. 2.10, though, and thus must be gained elsewise. The set of all 2^N CEs

$$\begin{aligned} E(\sigma_1) &= \sum_i V_i \Phi_i(\sigma_1) \\ E(\sigma_2) &= \sum_i V_i \Phi_i(\sigma_2) \\ &\dots \end{aligned}$$

can naturally be regarded as an $2^N \times 2^N$ equation system for the constants V_i which we can write in matrix form

$$\begin{pmatrix} E(\sigma_0) \\ E(\sigma_1) \\ \vdots \\ E(\sigma_{2^N-1}) \end{pmatrix} = \begin{pmatrix} \Phi_0(\sigma_0) & \cdots & \Phi_{2^N-1}(\sigma_0) \\ \Phi_0(\sigma_1) & \cdots & \Phi_{2^N-1}(\sigma_1) \\ \vdots & \ddots & \vdots \\ \Phi_0(\sigma_{2^N-1}) & \cdots & \Phi_{2^N-1}(\sigma_{2^N-1}) \end{pmatrix} \begin{pmatrix} V_0 \\ V_1 \\ \vdots \\ V_{2^N-1} \end{pmatrix} \tag{2.30}$$

The matrix, the *correlation matrix*, is nonsingular [11] due to the orthonormality of the cluster functions and can thus be inverted, yielding the values of the V_α.

However this is only useful and feasible, if the set af all 2^N ECIs can be reduced to a smaller set of the dominant interactions without neglecting a significant contribution to the CE (Eqn. 2.9), in other words if the CE exhibits *reasonable convergence behavior* and may be truncated. Then it is possible to interpolate from a few known input energies $E_{DFT}(\sigma)$ to all other σ, which was assumed in section 2.2. It is obvious that the number of inputs, N_{input}, must be as large as or larger than the number of desired ECI, N_{ECI}. The input energies might come from experimental measurement, but then N_{input} is rather small [16, 26], hence it is preferred to calculate the energies of a set of ordered configurations with DFT-methods. This procedure is referred to as the Connolly-Williams method [23] (cf. section 2.2), be N_{input} either equal (direct inversion) or larger than N_{ECI} (fitting methods). Since the CE is in principle exact the truncated CE is a valid method to conclude the properties of random configurations from a set of ordered configurations [26]. If two different input sets of the alloy system yield two different sets of ECIs this is an indicator of a weak choice of the truncation [24].

In addition to that the overall aim is using the CE to avoid computationally costly DFT calculations. If the ECI could only be achieved by solving the *full* equation system, the CE would be completely useless, since all $E(\sigma) = E_{DFT}(\sigma)$ would already be known. Moreover the question arises how to treat the infinite crystal.

The truncation of the CE is indeed possible (e.g. [16, 26, 31]) and thus one of the benefits of CE calculations over *ab initio* methods (DFT) is that the examination of a rather small set of input configurations allows us to extract predictions for *all* other configurations, whereas in direct DFT calculation each configuration must be treated independently. In that sense CE connects electronic structure calculations (DFT) with phase stability calculations [16].

2.6 Convergence

Before proceeding with convergence we examine the index set of the cluster series. In the most general formulation of the CE Eqn. 2.9,

$$E(\sigma) = \sum_{\alpha} V_\alpha \phi_\alpha(\sigma)$$

there is no obvious order on the index set α, neither have we imposed any order in the index set so far. It is indeed appropriate to sort the symmetry related clusters by their number of sites, i.e. their *order*, and by the distances between them, i.e. their *size*. The choice of the measure of size is not uniquely specified: for the pair clusters the length itself is somehow a mandatory and reasonable choice, but for three-dimensional polyhedra measuring the lengths w.r.t. to a barycenter might be more appropriate. A common measure of the size is the mean distance between the k sites of the cluster [32]. When we speak of convergence, we mean convergence w.r.t. both order and size, but we do not demand a strictly monotonic decrease of the ECIs [26].

As discussed before it is clear that the neglect of many terms is the condition for any practical use of the CE. The validity of the approximation, i.e. of the truncated CE, relies on the rapid convergence of the exact CE.

2.6.1 Heuristic Hints for the Convergence of the CE

Unfortunately there is no mandatory mathematical argument that the CE converges [4]. Physical intuition, though, suggests (e.g. Ref. [31]) that the ECIs fall off with distance, just as the electrostatic interaction between two charges falls off according to

$$V_{electrostatic}(r) \propto \frac{1}{r^2} \tag{2.31}$$

where r is the distance between them. In a multipole expansion of a charge distribution, the force falls off with an exponent which is the higher, the higher the moment is. Thus the contribution of clusters of smaller size should dominate over larger ones.

Following Ref. [32] we heuristically assume for a binary alloy that the pair interaction will converge to the mean value of the point energies for large distances, e.g.

$$E_{AB} = \frac{1}{2}(E_A + E_B) \tag{2.32}$$

for a system where site p is occupied by an A atom and p' by a B atom, respectively [32]. The ECI for the pair cluster $\alpha = (p, p')$ is:

$$\begin{aligned} V_{p,p'} &= \langle \sigma_p \sigma_{p'}, E(\sigma) \rangle \\ &= \frac{1}{2^N} \sum_{\sigma} \sigma_p \sigma_{p'} E(\sigma) \end{aligned}$$

There are 2^{N-2} configurations for each distinct occupation of (p, p'), which we denote σ_{AA}, σ_{AB} etc. and E_{AA}, E_{AB} is their respective average energy. Hence we have

$$\begin{aligned} V_{p,p'} &= \frac{1}{2^2} \frac{1}{2^{N-2}} \left[\sum_{\sigma_{AA}} E(\sigma_{AA}) - \sum_{\sigma_{AB}} E(\sigma_{AB}) - \sum_{\sigma_{BA}} E(\sigma_{BA}) \sum_{\sigma_{BB}} E(\sigma_{BB}) \right] \\ &= \frac{1}{2^2} (E_{AA} - E_{AB} - E_{BA} + E_{BB}) \end{aligned}$$

Under the assumption above (Eqn. 2.32) we obtain the result that the corresponding ECI vanishes:

$$\begin{aligned} V_{p,p'} &= \frac{1}{2^2}(E_{AA} - E_{AB} - E_{BA} + E_{BB}) \\ &= \frac{1}{2^2}\frac{1}{2}(2\ E_A - 2\ (E_A + A_B) + 2\ E_B) = 0 \end{aligned}$$

Analogously, for the triplet $\alpha = (p, p', p'')$ we have [32]

$$E_{ABB} \propto E_{AB} + E_B \tag{2.33}$$

and hence

$$\begin{aligned} V_{p,p',p''} &= \langle \sigma_p \sigma_{p'} \sigma_{p''} E(\sigma) \rangle = \frac{1}{2^N} \sum_{\sigma} \sigma_p \sigma_{p'} \sigma_{p''} E(\sigma) \\ &= \frac{1}{2^3}(E_{AAA} - E_{AAB} - E_{ABA} + E_{ABB} - E_{BAA} + E_{BAB} + E_{BBA} - E_{BBB}) \\ &= \frac{1}{2^3}(E_{AA} + E_A - E_{AA} - E_B - E_{AB} - E_A + E_{AB} + E_B \\ &- E_{BA} - E_A + E_{BA} + E_B + E_{BB} + E_A - E_{BB} - E_B) = 0 \end{aligned}$$

The heuristic argumentation that the CE is convergent was supported by the findings of early calculations of ECI. It was observed that the set of resulting ECIs featured some convergent behavior although resulting from more or less arbitrary truncation. Examples can be found in Ref. [26] for binary Pt alloys and lattice matched AlAs/GaAs semiconductor alloys.

2.6.2 The CE of the electrostatic Madelung energy

Zunger[26] illustrated the convergence behavior of the cluster expansion by applying it to the electrostatic Madelung Energy of a binary crystal

$$E_M(\sigma) = \frac{1}{2N} \sum_{i \neq j} \frac{Q_i Q_j}{|\mathbf{R_i} - \mathbf{R_j}|} \tag{2.34}$$

which can be calculated analytically. The indices i, j run over all N sites R_i of the lattice, which are either occupied by an A or a B atom and carry the net charge Q_i . The distance $|\mathbf{R_i} - \mathbf{R_j}|$ can be measured in therms of R, the nearest-neighbor distance in the lattice of interest. We use the binary basis set

$$\Phi_\alpha(\sigma) = \sigma_{p_{i_1}} \ldots \sigma_{p_{i_k}}$$

introduced before (Eqn. 2.21). In an ionic crystal all ions carry the same absolute charge, thus the effective charge of an ion depends on the sign of the charges of its neighbors. Following Ref. [26] we define a discrete model charge distribution depending only on its Z nearest neighbors

$$Q_i = \lambda \sum_{k=1}^{Z} \sigma_i - \sigma_k \tag{2.35}$$

where λ is a charge. This definition serves mainly for mathematical convenience. Calculations involving continuous charge distributions are in qualitative agreement [26]. According to Eqn. 2.10 the effective cluster interactions J_α of the CE of the Madelung Energy are

$$J_\alpha = \frac{1}{2^N} \sum_{\sigma} \Phi_\alpha(\sigma) E_M \tag{2.36}$$

Inserting E_M and Q_i it follows:

$$\begin{aligned} J_\alpha &= \frac{\lambda^2}{2} \frac{1}{2^N} \sum_{\sigma} \Phi_\alpha(\sigma) \sum_{i \neq j} \frac{1}{|\mathbf{R_i} - \mathbf{R_j}|} \sum_{k,k'=1}^{Z} (\sigma_i - \sigma_k)(\sigma_j - \sigma_{k'}) \\ &= \frac{\lambda^2}{2} \sum_{i \neq j} \frac{1}{|\mathbf{R_i} - \mathbf{R_j}|} \sum_{k,k'=1}^{Z} \frac{1}{2^N} \sum_{\sigma} \Phi_\alpha(\sigma)(\sigma_i - \sigma_k)(\sigma_j - \sigma_{k'}) \\ &= \frac{\lambda^2}{2} \sum_{i \neq j} \frac{1}{|\mathbf{R_i} - \mathbf{R_j}|} \sum_{k,k'=1}^{Z} \frac{1}{2^N} \sum_{\sigma} \Phi_\alpha(\sigma)(\sigma_i\sigma_j - \sigma_i\sigma_{k'} - \sigma_j\sigma_k + \sigma_k\sigma_{k'}) \end{aligned}$$

The products $\sigma_i\sigma_j$ etc. are basis functions $\Phi_\alpha(\sigma)$ themselves and due to the orthonormality we yield

$$J_f = \frac{\lambda^2}{2} \sum_{i \neq j} \frac{1}{|\mathbf{R_i} - \mathbf{R_j}|} \sum_{k,k'=1}^{Z} (\delta_{f,ij} - \delta_{f,ik'} - \delta_{f,jk} + \delta_{f,kk'}) \tag{2.37}$$

which are thus only nonzero if the clusters f are the pairs (i, j) etc. Note that for one choice of α, the other δ vanish: Let $\alpha = (i, k')$, then

> $\delta_{f,ij} = 0$ because k' is a neighbor of j and in particular $j \neq k'$,
>
> $\delta_{f,kk'} = 0$ because k is a neighbor of i and in particular $i \neq k$,
>
> $\delta_{f,jk} = 0$ because: $(i, k) \neq (j, k')$ because $i \neq j$ and $(i, k) \neq (k', j)$ because (i, k') was a pair $i \neq k'$

The exact expression for the J_α can be evaluated and compared to the ECIs of a truncated CE of the Madelung Energy gained by the Connolly-Williams method, as it was presented in Ref. [26] for binary fcc systems involving only the first five pair clusters. The numerical agreement [26] of the values of the J_α shows the rapid convergence of the CE even for the long range problem of the Madelung Energy.

2.7 Truncation

The macroscopic dimensions of metal specimens are by many magnitudes larger than typical atomic distances. For the treatment of bulk properties they are therefore described as infinite systems and all surface effects are neglected. For example the DFT calculations are performed for the infinite crystal [6], computationally realized by periodic boundary conditions. The Cluster Expansion for the infinite crystal, though, has infinitely many terms. Thus in addition to computational feasibility, as mentioned in section 2.5, truncation is in that sense conceptually necessary.

We had Eqn. 2.22

$$E(\sigma) = V_0 + \sum_p V_i \sigma_p + \sum_{(p,p')} V_i \sigma_p \sigma_{p'} + \sum_{(p,p',p'')} V_i \sigma_p \sigma_{p'} \sigma_{p''} + \dots$$

before; *truncation* refers to limiting the order of the clusters taken into account and truncating each term $\sum_p$, $\sum_{(p,p')}$, etc. We will use 'cluster selection' synonymously.

The truncation of the CE is a delicate problem and at least the choice of the lengths of the edges of the largest clusters to be considered is still largely arbitrary. The challenge is to select the 'right', i.e. dominant cluster interactions. Basically there are two approaches to select the clusters in a systematic manner, namely (1) hierarchically and (2) by a genetic algorithm.

2.7.1 An Hierarchical Approach to Cluster Selection

The hierarchical approach for the cluster selection [18, 31, 33] relies mainly on the heuristic arguments described above. There are two construction rules for the cluster set:

1) If a distinct cluster α_k is included, then all its subclusters must be included.

This mirrors the observation that the energy of a system contains all subsystems' energies, may they interact or not [31].

2) If a cluster of a certain size is included, then all smaller clusters of the same order must be included.

We have exemplified before that – heuristically – the ECI vanish when moving one site p to infinite distance from the other sites it is supposed to interact with, cf. 2.6.1.

2.7.2 Using a Genetic Algorithm for Cluster Selection

The Genetic Algorithm (GA) for the cluster choice [17, 34] is a systematical iteration procedure with little arbitrary conditions and is nowadays the commonly preferred method for the cluster selection. We give a short overview of the basic concept.

Evolutionary (or genetic) algorithms [17, 34] are a well known concept in computer sciences, with many successful applications also in physics. They are particularly efficient tools to tackle large and/or highly correlated search spaces [17]. This is certainly the case for the cluster selection, as the number of possible clusters is in principle 2^N, only diminished due to lattice symmetry, cf. sections 2.3 and 2.4.

GAs are designed to mimic biological evolution ('survival of the fittest') using random 'mutations', in contrast to classical iterative approximation algorithms like, say, Newton's method [35], where – roughly spoken – the same equation is evaluated taking the result of the preceding iteration as a new input. Classical approaches like Newton's method are often restricted to continuous search spaces and to the calculation of the solutions of a known model equation. For the case of CE, GAs are used [17, 34] for *model selection* – as the main question arising for the construction of an accurate yet truncated CE is: 'Which many body interaction terms or ECI are physically important?'

The systematical evaluation of all possible choices of 'some' clusters out of an even limited (in terms of size and order) set of clusters (cluster pool) is practically intractable. Some authors speak of a 'combinatorial explosion' [34] to point out the excessive increase of possibilities even when adding only one or two clusters to the pool, since the number of distinct choices of k clusters out of a pool of n is given by the binomial coefficient

$$\binom{n}{k} = \frac{n!}{k!(n-k)!} \tag{2.38}$$

and hence the number of all cluster choices within this cluster pool is the sum over $k \leq n$. Furthermore this search space is highly correlated, as the combined use of two particular clusters result in a sufficiently accurate CE while using one of them alone may not [34].

We present the basic idea of the GA as it was presented in [17, 34], more details can be found in Ref. [17].

- The cluster pool is the set of all clusters which are taken into account for selection. It should be as general as possible and obey no particular selection rules. In particular it should include clusters much larger than possibly suggested by the researcher's intuition. Let the elements of the pool be consecutively numbered, with no particular order. Let their total number be n.

- Each cluster choice is represented by an n-dimensional vector ('genome') consisting of 1 and 0 ('genes'), where the entry 1 (0) at index i means that cluster i is included (not included) in the cluster choice. In principle one might set a maximum number of active genes per genome, for details see Ref. [17]. The set of different genomes in one iteration ('generation') is called a population, with population size N_{Pop}. The population should be large enough that each individual gene occurs at least in two genomes in the initial population [17].

- The cross validation score (CVS, e.g. [17, 19, 31, 34, 36, 37]) is invoked as 'fitness criterion'. It is a measure of the predictive power of the CE and will be described in the following chapter. A certain part of the population with a 'high fitness' is retained in the next generation, while the remaining are 'mated' and replaced by their 'children'.

- Two randomly selected genomes are mated to create a child generation. Each gene of the child genome is individually inherited from either parent, the probability is related to the relative fitness of the parents. This mimics the heredity of the 'better' or 'fitter genetics' in biological evolution. Additionally, each gene can 'flip'[17] after mating with a certain probability ('mutation rate').

- The evaluation of the fitness of the present generation and the creation of the successive generation are repeated iteratively until no further improvement of the fitness can be achieved. Since it is not possible to judge whether the global optimum has been found or whether the algorithm is trapped in a local minimum, the procedure is repeated several times with a new random initial population or by a dramatic increase of the mutation rate ('lock-out strategy'). Among the so-gained near-optimum solutions the one exhibiting minimal CVS is picked as the cluster set of the CE.

One of the first applications of the GA in Ref. [17, 34] illustrates particularly well the progress achieved by excluding intuition as far as possible when searching for stable structures of an alloy system. The GA was applied to the calculation of the CE of the bcc Ta-W system. The resulting phase diagram shows that the actual ground states are significantly lower in energy than the *usual suspects*. The CE optimized by the GA allowed to systematically calculate the accurate energies of many more configurations than only the *usual suspects*.

2.8 Calculating the ECIs

To achieve a robust CE with high predictive power for the energies of new configurations of the alloy system the ECIs are calculated by iteratively solving the overdetermined equation system

$$\begin{pmatrix} E(\sigma_1) \\ E(\sigma_2) \\ \vdots \\ E(\sigma_n) \end{pmatrix} = \begin{pmatrix} \Phi_1(\sigma_1) & \cdots & \Phi_l(\sigma_1) \\ \Phi_1(\sigma_2) & \cdots & \Phi_l(\sigma_2) \\ \vdots & \ddots & \vdots \\ \Phi_1(\sigma_n) & \cdots & \Phi_l(\sigma_n) \end{pmatrix} \begin{pmatrix} V_1 \\ V_1 \\ \vdots \\ V_l \end{pmatrix} ,$$

varying the input set in every iteration loop. A comprehensive description of the iterative fitting routine can be found in Ref. [16, 37, 38].

Note that for a set of n linearly independent equations of the same number $l = n$ of parameters there is always an exact unique solution, yet it is not possible to make any predictions if the values of the parameters would also describe the $n + 1$ equation sufficiently correctly. This is the aim of the CE, though. For that purpose it is more apt to solve the overdetermined equation system $n > l$ with traditional least squares methods or to minimize the error function w.r.t. the *Cross Validation Error* or *score* (CVS) (e.g. [17, 19, 31, 34, 37]), which we describe in more detail below. For now we just mention that the CVS is a measure of the ability of a fitted model equation to accurately predict data points not included in the fit. In other words the CVS is a measure of the predictive power of the truncated CE.

The initial input set contains the so-called usual suspects – physical ground states (if existing), configurations of high symmetry – and superlattice configurations (SL, see below). For this input set a CE is calculated, i.e. the overdetermined equation system is solved. The standard procedure nowadays includes a GA-cluster selection, while the input set is unchanged (*'inner loop'*, [37]). This 'trial CE' is then used for a ground-state search: $E_{CE}(\sigma)$ is calculated for all configurations up to a certain (arbitrary) unit cell size. The convex hull of the corresponding formation enthalpies,

$$\Delta E(\sigma, A_m B_n) = \frac{1}{m+n} \left[E(\sigma, A_m B_n) - m \; E(\sigma, \text{pure A}) - n \; E(\sigma, \text{pure B}) \right] \quad , \tag{2.39}$$

is the ground-state line. If new ground-states (i.e. ones that were not included in the input set) are found, they are included in a new input set, as well as configurations with energies near the ground-state line. In addition to that, for each input configuration it is checked if the omission will change the ECIs – if not, the configuration is excluded from the input set. Note that for all new input configurations the DFT energies must be calculated.

These calculations are repeated for the new input set (*'outer loop'*, [37]) until the CE-ground-state-line is stable. The phase diagram for $T = 0K$ is obtained as a side effect of this procedure and another benefit of the CE compared to ab-initio methods alone.

We emphasize again: Due to its low computational cost the CE can search a much larger subset of the configuration space than DFT, e. g. systematically search all possible configurations up to a certain number of atoms in the unit cell, and is therefore less likely to miss the physical ground state for $T = 0K$.

Remark: Alternative Methods to Determine the ECI

The ECIs can be extracted empirically by fitting to known features of the phase diagram, such as critical temperatures [26]. This is a pragmatic but very simplistic approach, yielding hardly new information of the alloy system. Further, ordered configurations might be treated as a perturbation of the random alloy for which *ab initio* model calculations ca be performed. There are also methods to directly calculate the expansion coefficients V_i according to 2.10, using appropriate model Hamiltonians (Direct Configural Averaging, Coherent Potential Approximation). [10, 16, 26, 39]

The Connolly-Williams method sketched above – fitting the V_i to a set of ordered configurations – with its many adaptions is the preferred method today. It is applicable to a wide range of alloy systems and preserves the accuracy of the DFT input calculations. Descriptions of state of the art implementations are given in refs. [19, 37].

2.9 Relaxations

In real multicomponent crystalline structures the atomic positions deviate from the ideal cubic lattice, i.e. the unit cell volume, the unit cell vectors (crystallografically: the primitive vectors) and the position vectors of the atoms in the unit cell (crystallografically: basis vectors) would differ from the respective values on the ideal lattice and 'relax'. This is particularly the case for, but not restricted to, lower symmetry configurations such as $L1_0$ or DO_{22} of size-mismatched constituents, coherent superlattices and alloys consisting of hydrostatically stiff constituents [26].

Relaxation leads to a change in the internal energies, formation enthalpies, etc. and has noticeable effects on electronic structure and on phase stability and thus on the phase diagram [26].

The implementation of the CE such as applied to *ideal lattice* is still valid: the crystals energy is still a unique property of the configuration. In that sense the term 'cluster' or 'figure' has rather topological than geometric meaning. Experience showed that it nevertheless leads to a slower convergence compared to unrelaxed input sets. Neglecting relaxation, though, negatively affects the predictive power of the CE, yet it was neglected in the beginning of this field. Concerning the calculations of Connolly and Williams [23], relaxation effects stayed unnoticed due to the high symmetry of the configurations of the input set. [26]

2.10 Coherent Superlattices

A binary coherent superlattice (SL) is a configuration consisting of stacks of pure A and pure B where certain numbers ('periodicity') of pure A planes and pure B planes are orientated perpendicular to the same crystallographic direction $[h, k, l]$ within one distinct Bravais lattice. The definition for more than two constituents is analogous. [26] Without loss of generality we restrain the discussion to superlattices of the type A_nB_n where n is the periodicity of the SL.

Experience [16, 26] shows that CEs from unrelaxed input sets fail to describe the configurational energy of SLs even for short periodicity. Moreover any finite CE must fail in this case [16, 26, 40]: For $n \to \infty$ the system's formation enthalpy goes to the *constituent strain (CS) energy*, which is due to the lattice mismatch of the pure constituents and depends on the orientation (h, k, l) of the planes. In the limit $n \to \infty$, though, the finite clusters originating from any A atom are cluster in bulk A. The CE hence treats the crystal as a whole as bulk A and thus yields $\Delta H \to 0$.

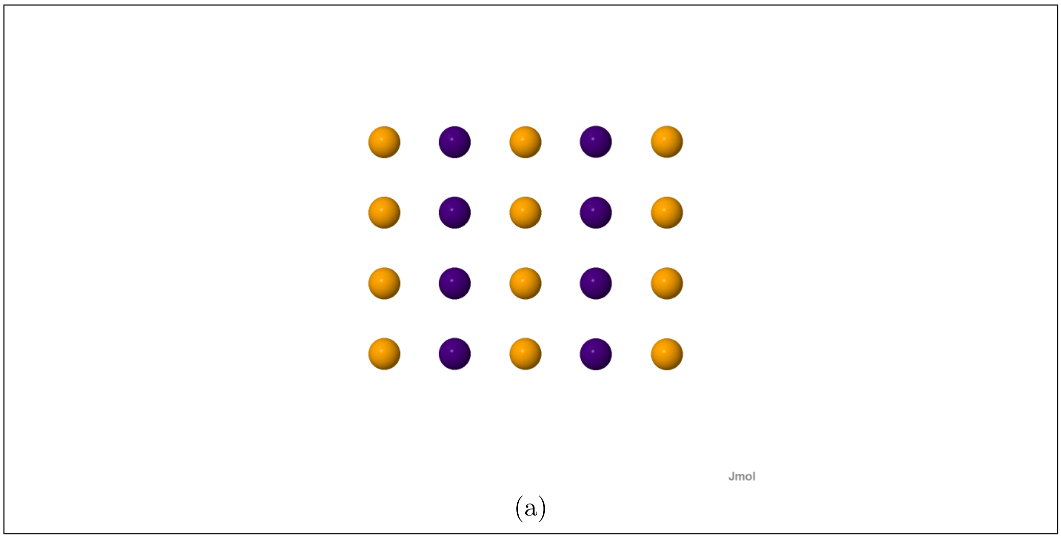

(a)

Figure 2.7: A two-dimensional lattice superlattice of periodicity $n = 1$.

2.11 Mixed Space CE

The reciprocal space CE was introduced in order to deal with weak convergence behavior of CE of fully relaxed input sets and the failure to correctly describe the configurational energies of SLs [16, 26, 38, 40]. The basic idea of the reciprocal space or mixed space CE (MSCE) is to use one single smooth [26, 38] reciprocal space function $J(\mathbf{k})$ in lieu of infinitely many J_f. A function $J(\mathbf{k})$ over few $\mathbf{k}$ corresponds to an infinite series in real space [26, 38] and circumvents somehow arbitrary truncation.

According to Refs. [26, 40] this is only done for the pair interaction

$$E_{pair}(\sigma) = N \sum_{\mathbf{k}} J_{pair}(\mathbf{k}) |S(\mathbf{k}, \sigma)|^2 \tag{2.40}$$

with the Fourier transforms $J_{pair}(\mathbf{k})$ and $S(\mathbf{k}, \sigma)$

$$S(\mathbf{k}, \sigma) = \frac{1}{N} \sum_{l=1}^{N} \sigma_l(\sigma) e^{i\mathbf{k}\mathbf{p_l}} \tag{2.41}$$

of their respective real space functions. $\mathbf{p_l}$ are the real space coordinates of the unrelaxed lattice sites p_l. For ordered configurations the functions $S(\mathbf{k}, \sigma)$ are nonzero only for a finite set of $\mathbf{k}$, viz for $\mathbf{k} = 0$ and reciprocal lattice vectors $\mathbf{k}$ of the unit cell of σ and hence Eqn. 2.40 is a finite sum in $\mathbf{k}$-space. The mentioned smoothness criterion automatically 'selects' the dominant pair interactions and means in principle that the magnitudes of the effective pair interactions fall off rapidly with distance. [26, 40]

All terms in in the CE Eqn. 2.9 can be transformed to **k**-space, but this is needlessly complicated [26], thus the many-body interaction terms (MBIT) are treated in real space. The GA [17, 19, 34, 37] is a powerful tool for the selection of the MBITs.

The MSCE roughly sketched here does not correctly describe the CS energy, which has to be treated separately. Hence overall the (MS)CE for the formation enthalpy is [40]

$$\Delta H_{CE}(\sigma) = E_{pair}(\sigma) + E_{\mathrm{MBIT}}(\sigma) + E_{CS}(\sigma) \tag{2.42}$$

where $E_{MBIT}(\sigma)$ denotes a real space CE, i.e. the truncated sum over the other clusters in Eqn. 2.9. $E_{CS}(\sigma)$ can be gained from continuum elasticity theory. The computational procedure to calculate the correct MSCE (including constituent strain) in general and $J_{pair}(\mathbf{k})$ in particular is described in Ref. [40].

2.12 The Treatment of Vacancies in Solids: The Local Cluster Expansion

Locally restricted properties of the solid located around a distinct lattice site p_i can be treated as a perturbation of the global property within the framework of the Local Cluster Expansion (LCE) [4, 13–15]. Of particular interest are dilute vacancies. The formation enthalpy of a vacancy at site i depends solely on the occupation of the neighboring atomic sites [13]. It is clear that local properties, such as the random occurrence of an isolated vacancy in the solid, show no translational symmetry and thus [14] the *point group* of the lattice is the relevant symmetry operation of the LCE [4, 14] around the site of interest. The LCE therefore includes only classes of clusters α_i that are symmetric with respect to the point group of site i (indicated by the index i in α_i).

$$g_{\mathrm{local}}(\sigma) = \sum_{n=\alpha_i} J_n \xi_n(\sigma) \tag{2.43}$$

The ξ_n are the cluster functions introduced above and the J_n are the *local effective cluster interactions*, LECIs, analogous to the ECIs. To clarify this we describe the LCE for vacancies in greater detail.

For the treatment of dilute vacancies in binary alloys we introduce an *effective vacancy formation enthalpy* ΔE_i^{eff} [13]

$$\Delta E_i^{eff} = E_i^V(\sigma) - \frac{1}{2}\left[E_i^A(\sigma) + E_i^B(\sigma)\right] \tag{2.44}$$

a purely mathematical auxiliary tool with no direct physical meaning. $E_i^V(\sigma)$ is the energy of the solid of configuration σ with a vacancy occupying site i, while $E_i^A(\sigma)$ and $E_i^B(\sigma)$ are the energies when site i is occupied by an A-atom or B-atom, respectively.

ΔE_i^{eff} does not depend on whether site i is occupied by an A or a B atom: $E_i^V(\sigma)$ itself naturally does not and $\frac{1}{2}(E_i^A(\sigma) + E_i^B(\sigma))$ as an average neither does. That means ΔE_i^{eff} does only depend on the local occupations around site i and can be described by an LCE [13]. The averaged term can be calculated by the binary CE. The computationally hard and physically interesting term, the internal energy of the binary solid containing one vacancy located at site i, then reads

$$E_i^V(\sigma) = \underbrace{\Delta E_i^{eff}}_{\text{LCE}} + \underbrace{\frac{1}{2}\left[E_i^A(\sigma) + E_i^B(\sigma)\right]}_{\text{binary CE}} \quad , \tag{2.45}$$

and can be conveniently calculated with cluster expansion methods once the ECI and LECI are determined. Hence for dilute vacancy concentrations the use of the ternary CE is elegantly avoided by summing a binary CE and a LCE.

For the vacancy-LCE the sum in Eqn. 2.43 goes over clusters around site i, but not containing site i itself [13], up to a certain truncation.

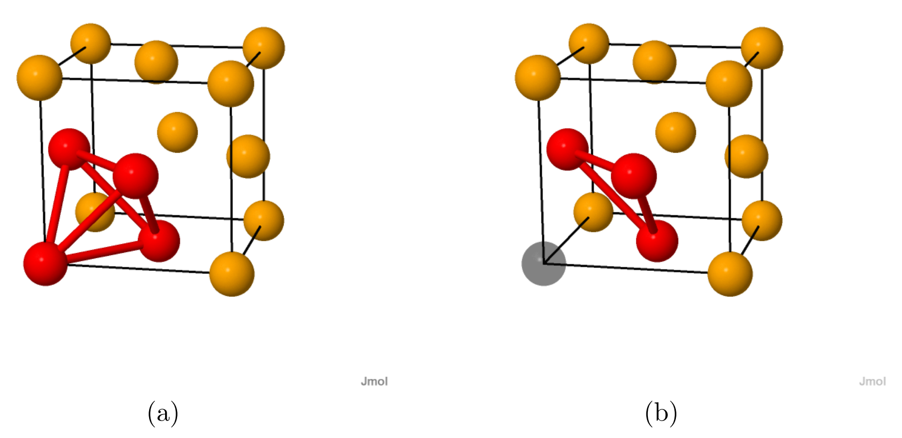

(a) (b)

Figure 2.8: Clusters for the LCE: (a) the tetrahedron, (b) the LCE 'tetrahedron'.

This can also be seen as taking clusters originating from the vacant site i, e.g. the NN-pair, other pairs, the NN-triangles, etc. and deleting site i from each of them, as illustrated in Figure 2.8. We therefore denote the LCE point cluster originating from the NN-pair *the NN-pair cluster*, etc.

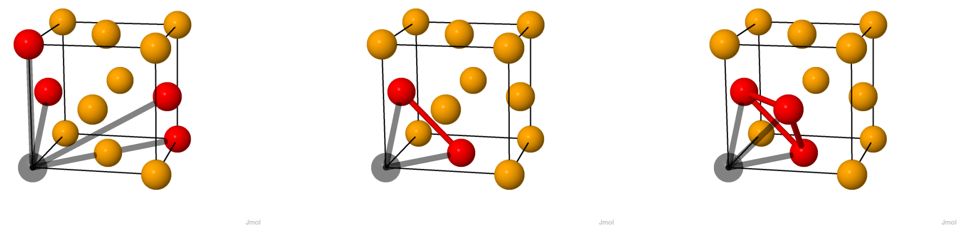

(a) (b) (c)

Figure 2.9: The LCE clusters. (a) LCE-pair, (b) LCE-triangle, (c) LCE-tetrahedron. From [13]

Figure 2.9 shows the clusters for the LCE of the fcc Al-Li-system used for introduction of the LCE for the treatment of vacancies in Ref. [13].

We note that for a near-optimum cluster selection the same methods as for the CE are applicable (section 2.7) [41]. Furthermore the requirement to explicitly exclude vacancy-vacancy interactions justifies heuristically the truncation of the LCE within few neighboring shells.

For the calculation of the LECIs three input energies for each configuration are necessary: $E_i^V(\sigma)$, $E_i^A(\sigma$ and $E_i^B(\sigma)$, cf. Eqn. 2.44, usually calculated by means of DFT. To reflect the lack of vacancy-vacancy-interactions the calculation cells need to be sufficiently large, at least $3 \times 3 \times 3$ conventional unit cells, which is equivalent to 108 atomic sites (or 107 atoms plus one vacancy). Internal relaxations have to be taken into account, while leaving the total volume constant [13].

The so-gained expansions for the terms in Eqn. 2.45 may be used in MC simulations, promising similar accuracy as *ab initio*-MC at greatly reduced computational effort.

The LCE was also successfully employed to the calculation of activation barriers for diffusion within transition state theory[2] in [4, 42, 43], to multicomponent systems where vacancies remain on one sublattice [42, 43] or to local vibrational modes [14, 15].

Chapter 3

Documentation of the Computational Methods

The calculation of the ECIs and LECIs through the Connolly-Williams method can be divided into three computationally independent parts, described in detail below:

- Preparations: Choice of configurations (for both input set and testing), calculation of their energies (DFT), and choice of clusters
- Calculation of the correlation functions
- Calculation of the (L)ECI, i.e. solution of the of the equation set 2.30

These three steps may alternate during the fitting process. We find it convenient to create a kind of database of configurations and their correlation functions for a relatively large set of clusters, in order to easily vary the input set and clusters of the equation set 2.30 for the (L)ECI. Moreover we believe that this approach brings about a clearer structure of the algorithm, as the calculations are done under the same controlled conditions.

In the following we describe the calculation of the LECIs for the Ni-Al-alloys with Ni concentration near the stoichiometry of Ni_3Al.

3.1 Preparations

3.1.1 Configurations

We aim to describe vacancy mediated atomic migration in $L1_2$ and $D0_{22}$ Ni_3Al. Therefore we restrict the input set for the calculation of the effective cluster interactions of the LCE (LECI) to configurations close these configurations, i.e. some $L1_2$ and $D0_{22}$ structures with antisite defects with unit cells of $3 \times 3 \times 3$ conventional fcc unit cells (108 atoms) with an isolated vacancy (V) at the center (lattice site i). We note that for each configuration three variants are needed (cf. 2.12) – V at site i, Ni at site i and Al at site i – since the effective vacancy formation enthalpy $\Delta E_{V,i}^{eff}$ is (Eqn. 2.44)

$$\Delta E_i^{eff} = E_i^V(\sigma) - \frac{1}{2}\left[E_i^A(\sigma) + E_i^B(\sigma)\right] \quad .$$

Due to the large computational effort for the *ab initio* energy calculations for large unit cells we have only a rather small set of configurations at our disposal. The energies of 14 such Ni_3Al defect configurations, i.e. all three variants for each of the 14, were calculated using VASP[44–48] and kindly provided to the author of this work by Martin Leitner[49]. The configurations are listed in the Appendix.

3.1.2 Clusters

The cluster functions of the LCE differ from the cluster functions of the global CE (cf. 2.12). Instead of all clusters in the crystal only the clusters symmetric w.r.t. the point group are taken into account, i.e. all clusters share one lattice site (the site of the vacancy). For the V-LCE these are clusters *surrounding but not containing* the atom of interest at site i. In other words each k-cluster containing site i is now reduced to an $(k-1)$-cluster by the omission of site i. As mentioned before we refer to them *including* site i, though, e.g. *nearest-neighbor triplet* refers to the NN-pair which is left after removing site i from the triangle.

Figures 2.9 and 3.1 show the clusters of the cluster pool for the calculation of the LECI. We consider the clusters of the nearest-neighbor tetrahedron approximation (NN-pair, NN-triplets, NN-tetrahedron), the remaining pairs in the conventional fcc unit cell (clusters nos. 2-7) and several additional clusters (nos. 8-28) up to the order of 4 and up to half V-V distance, i.e. half lattice parameter of the defect configuration; plus the *null cluster* (cluster no. 1) with $\xi_0(\sigma) = 1 \ \forall \sigma$. The clusters are relatively small to reflect the assumption of no V-V interaction.

For a quick and easy calculation of the correlation function (cf. sections 3.2 and 3.4.1) a list of the coordinates of the vertices of all symmetric clusters (symmetric w.r.t. the point group O_h) was created (*mask*) for each cluster of a kind. The value of one particular LCE correlation function can be obtained by calculating the corresponding binary correlation function with $\sigma_i = 1$. This is equivalent to multiplying each addend in the formula of the

Table 3.1: The cluster pool for the LCE I

Clusters (1) (null cluster) - (7) cf. 2.9		
(8)	(9)	(10)
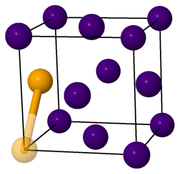	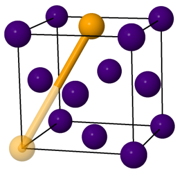	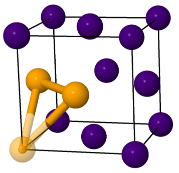
$(0, 1, 1)$	$(1, 2, 1)$	$(-1, 0, -1)$ $(0, -1, -1)$
(11)	(12)	(13)
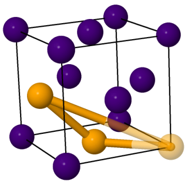	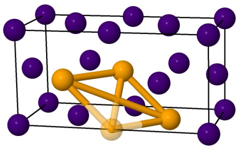	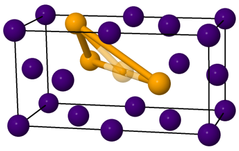
$(-2, 1, 1)$ $(-1, 1, 0)$	$(-1, 0, 1)$ $(0, 1, 1)$ $(1, 1, 0)$	$(-1, 0, 1)$ $(-1, 1, 0)$ $(1, -1, 0)$
(14)	(15)	(16)
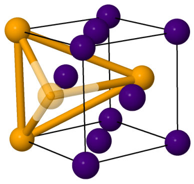	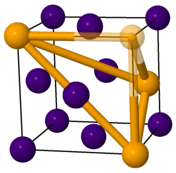	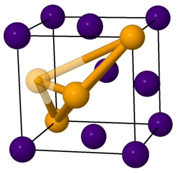
$(-1, 0-, 1)$ $(-1, 0, 1)$ $(0, 2, 0)$	$(-2, 0, 0)$ $(0, 0, -2)$ $(0, 1, -1)$	$(0, 1, -1)$ $(1, -1, 0)$ $(2, -1, 1)$

Table 3.1: The cluster pool for the LCE II

(17)	(18)	(19)
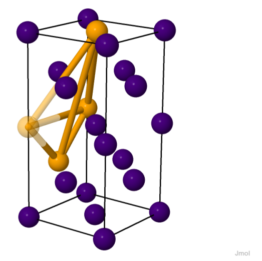	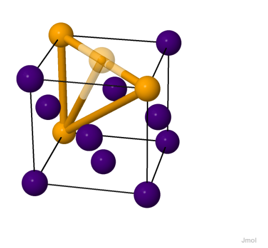	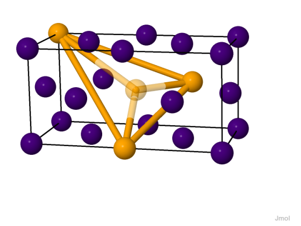
$(0, 1, -1)$ $(0, 2, 0)$ $(1, 1, 2)$	$(-1, 1, -2)$ $(-1, 1, 0)$ $(1, -1, 0)$	$(-2, 1, 1)$ $(0, -1, -1)$ $(1, 1, 0)$
(20)	(21)	(22)
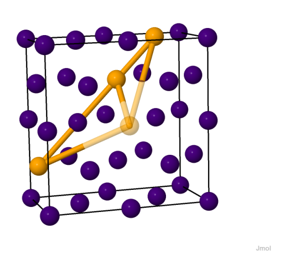	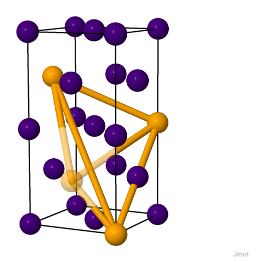	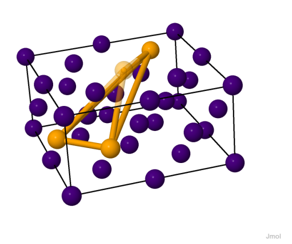
$(-2, 1, -1)$ $(0, 1, 1)$ $(1, 1, 2)$	$(-2, 1, 1)$ $(-1, -1, 2)$ $(0, 1, -1)$	$(0, 1, -1)$ $(1, -2, 1)$ $(1, -1, 2)$
(23)	(24)	(25)
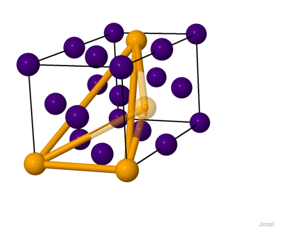	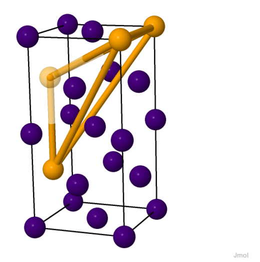	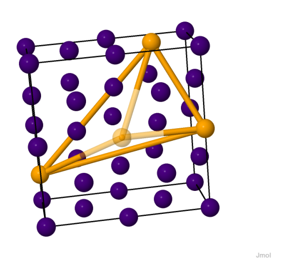
$(0, 1, -1)$ $(1, -2, 1)$ $(2, 1, -1)$	$(-1, -2, 1)$ $(0, 0, -2)$ $(1, -2, 1)$	$(0, -2, 0)$ $(1, -1, 2)$ $(1, 2, -1)$

Table 3.1: The cluster pool for the LCE III

(26)	(27)	(28)
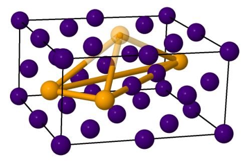	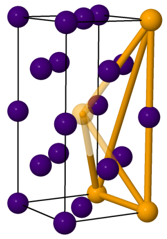	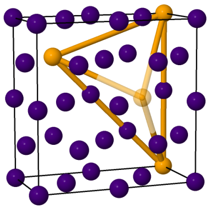
$(1,-2,-1)$ $(1,-1,-2)$ $(1,1,2)$	$(-2,-1,1)$ $(2,-1,1)$ $(2,1,1)$	$(-2,1,1)$ $(1,-1,2)$ $(1,1,-2)$
$a_{fcc} = 2$. The shaded atom is a vacancy at (0,0,0). All lattice boxes are rotated such that the cluster is better visible.		

corresponding LCE correlation function with +1, leaving the value itself unchanged. Contrary to the calculation of the binary cluster functions (section 3.4.1), where all symmetric clusters originating from any of the basis atoms are summed up, only clusters originating from the vacancy are evaluated. However, this ansatz allows us to use the same masks and even the same algorithm, slightly adapted, for both the CE and the LCE.

3.2 Calculation of the LCE Correlations

Each lattice configuration is represented by a three-dimensional array $Lattice(x, y, z)$ whose indices (x, y, z) refer to the coordinates within the calculation cell. The array itself, i.e. the array elements with their discrete integer indices, represents a simple cubic lattice with lattice parameter $a_{\text{simple cubic}} = 1$, hence the lattice parameter of pure fcc is $a_{\text{fcc}} = 2$. In order to represent an fcc configuration its entries are

- $Lattice(x, y, z) = 0$ if (x,y,z) does not represent an fcc lattice vector,
- $Lattice(x, y, z) = 1$ if (x,y,z) is occupied by Ni or
- $Lattice(x, y, z) = -1$ if (x,y,z) is occupied by Al, respectively.

Hence for the Ni and Al sites the corresponding array entry is the spin variable, itself. To be precise, this array is just a modification of the configuration vector σ introduced in section 2.1, where we implicitly have consecutively enumerated the lattice sites p.

For the calculation of the value of one particular ξ_f function of one configuration we simply multiply the occupation variables at the coordinates of the vertices of each specific cluster in f, i.e. the corresponding entries in $Lattice(x, y, z)$. The mean value of these spin products of the symmetric clusters is the value of the corresponding correlation function.

The values of the cluster functions for each configuration are stored in a two dimensional array (*correlation matrix*, cf. section 2.5) together with the ΔE_i^{eff}. For a certain cluster selection from the cluster pool the submatrix consisting of the corresponding columns of this correlation matrix is used for the calculation of the LECI.

3.3 Calculation of the LECI

We can now set up the set of equations to calculate the LECI

$$\Delta E_i^{eff} = correlationmatrix \cdot LECI \tag{3.1}$$

MatLab is used for the quick and convenient solution (least squares procedure) of the matrix equation with no further matrix manipulations. It is of course possible to realize the calculations as a Fortran program using linear algebra libraries such as LAPACK. But since the correlations, which are the coefficients in the linear system of equations (cf. Eq. 3.1), differ by several orders of magnitude (they can only take values between -1 and 1 but their absolute values can be magnitudes smaller – this is particularly the case for the global binary CE) further matrix manipulations such as preconditioning are required. For further details we refer to the standard literature of numerics [50]. MatLab is optimized for the numerical solution of large systems of equations and delivers the solution without further user input.

We use 11 of the 14 input configurations as input set and the remaining three (nos. 6, 10, 11, cf. Figure 3.1) as test set.

As a first approach we use the clusters used in Ref. [13], the first paper about LCE for vacancies: the pairs in the conventional fcc unit cell, the NN-triangle and the NN-tetrahedron plus the null cluster. This set of clusters is the simplest choice. Nevertheless we find the correlation matrix to be rank deficient with $r = 4$ while full rank $r = 7$, which means we obtain only four independent LECI. These four LECI reproduce the input set reasonably well but fail to fulfill important quality criteria such as preserving the the order of the energies and making sufficiently accurate predictions for the test configurations.

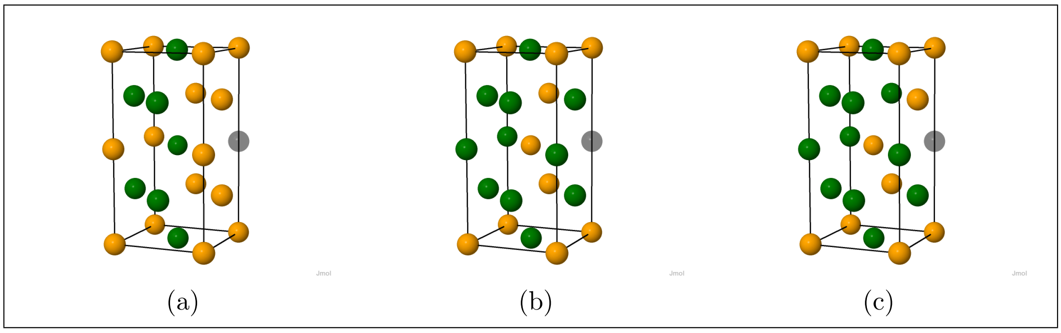

(a) (b) (c)

Figure 3.1: The test set. (a) $L1_2$ configuration no. 6, with Al vacancy, (b) $D0_{22}$ configuration no. 10, with Ni vacancy, (c) $D0_{22}$ configuration no. 11, with Ni vacancy. Ni: green, Al: yellow. The shaded atom is the vacancy, which is located at the center of the calculation cell.

To identify which four clusters are linearly independent we checked the rank of all $\binom{7}{4}$ possible choices. There are nine sets of four clusters such that $r = 4$. Since all calculated LCEs are likewise imprecise we aimed to obtain seven linearly independent clusters and modified the cluster set.
In principle we need to check all $\binom{21}{7}$ possible choices, but for simplicity we make an educated guess for a starting cluster set: Some configurations have anti-site defects in the first shell around the vacancy. Therefore we choose a 4-out-of-7 set from above containing the NN-pair and the NN-tetrahedron – the NN-triangle and the NN-tetrahedron are linearly dependent for this set of configurations – viz. the set $\{1, 2, 5, 7\}$. We consider this approach to be reasonable but indeed arbitrary.

For all 70 possible choices for the remaining three *linearly independent* clusters we calculate the LECI and the leave-one-out-CVS (since 11 is a prime number, see below). The respective cluster sets are listed in the appendix.

An iterative procedure as it is the present standard for the calculation of a (binary) cluster expansion (cf. 2.8) does not seem advantageous: In contrary to usual CE calculations we work in a narrow concentration range, where there are no physical ground states at the end points of the concentration interval and due to the large computational effort for first principles calculations for large unit cells we have only few configurations at our disposal. LCE literature [4, 13–15, 42, 43, 51] provides no such instruction, neither.

For all 70 LCEs the energies ΔE_i^{eff} of the three test set configurations are calculated and compared to their *ab-initio* value.

3.4 Some Details on the Computational Procedure of the Binary CE

3.4.1 The calculation of the Cluster Functions

We have introduced the well established notation for the infinite crystal before:

$$\begin{aligned}\overline{\Pi}_f(\sigma) &= \frac{1}{ND_f}\sum_{\alpha\in f}\Phi_\alpha(\sigma)\\ E(\sigma) &= N\sum_f D_f V_f \overline{\Pi}_f(\sigma)\end{aligned}$$

For the calculation of the correlation functions of configurations of which the crystallographic bases contain more than one basis atom, though, we find it more convenient to adapt the formulae. Let N now denote the number of unit cells and m the number of atoms in each of the cells. Hence $Nm = N_p$ is the number of sites in the lattice. Let f' be the set of clusters α' symmetric w.r.t. the point group of p. We write:

$$\begin{aligned}E(\sigma) &= \sum_i V_i\Phi_i(\sigma)\\ &= \sum_f V_f\sum_{\alpha\in f}\Phi_\alpha(\sigma)\\ &= \sum_f V_f \sum_{\text{unit cells}}\sum_{p\in\text{basis}}\sum_{\alpha\in f'}\frac{1}{k_\alpha}\Phi_\alpha(\sigma)\end{aligned}$$

as we have mentioned in section 2.4. The summation over all unit cells and all basis atoms is of course equivalent to sum over all lattice sites p. Hence

$$\begin{aligned}E(\sigma) &= N\sum_f V_f\frac{1}{k_\alpha}\sum_{p\in\text{basis}}\sum_{\alpha\in f'}\Phi_\alpha(\sigma)\\ &= Nm\sum_f V_f\underbrace{\frac{1}{k_\alpha}\frac{1}{m}\sum_{p\in\text{basis}}\sum_{\alpha\in f'}\Phi_i(\sigma)}_{D_f\overline{\Pi}}\quad .\end{aligned}$$

In order to calculate the the values of the cluster functions for each σ we find it more convenient to implement

$$\frac{1}{k_\alpha}\frac{1}{m}\sum_{p\in\text{basis}}\sum_{\alpha\in f'}\Phi_\alpha(\sigma) = D_f\overline{\Pi}(\sigma)$$

which are the elements of the correlation matrix itself.

3.4.2 Further Procedure

We implemented a simplified procedure, compared to the described state-of-the-art methods for Connolly-Williams inversion.

- Initialize: Choose a random set of 60 configurations out of a pool of 300. The DFT(VASP) energies of these 300 configurations were kindly provided to the author of this work by Martin Leitner[49].
- Calculate the ECIs for some random sets of 30 clusters out of a pool of 50, proceed with the CE with the smallest CVS.
- Calculate $E_{CE}(\sigma)$ for all configurations, find the ground-state line. All new ground states and configurations near the ground-state line are included in the new input set.
- Re-calculate the ECIs.
- Repeat until the ground-state line is stable.

Although the thus obtained CE has a small CVS the ground-state line does not reflect the physical ground-states. Figure 3.2 shows the calculated phase diagram. The diamonds are the DFT energies of the ground states and the full line is the respective ground-state line, the squares and the dotted line represent the calculated ground-state line. Narrowing the concentration range to $c_{Ni} \approx 0.75$ did not substantially improve the results.

3.5 Cross Validation

In the following we give a brief description of cross validation. Further details can be found in [17, 19, 31, 34, 36, 37].

We start with a model equation, in our case: the set of clusters, and set of N 'measuring points', in our case: the input set. The variables of the model are fitted to the inputs, i.e. the ECI are calculated. The fitting error is a measure of the accuracy of the fit and can in principle be eliminated by the use of the same number of variables and inputs. Yet it provides no information on the accuracy of predictions. Thus we divide the input set into k disjoint subsets of N/k elements,

$$\{\sigma_1, \ldots, \sigma_N\} = \{\sigma_1, \ldots, \sigma_{\frac{N}{k}}\} \cup \ \ldots \ \cup \{\sigma_{(k-1)\frac{N}{k}+1}, \ldots, \sigma_N\} \quad .$$

Then we use each subset as *test set*: The model is fitted to the union of the remaining $k-1$ sets and the mean squared deviation of the test set is

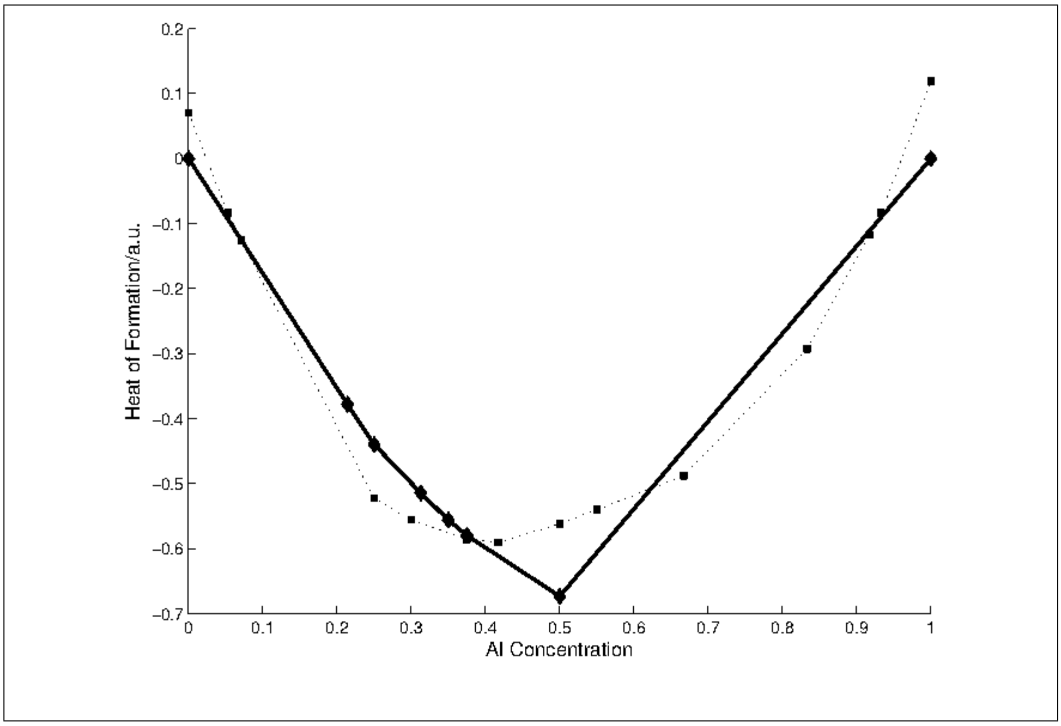

Figure 3.2: Calculated Ni-Al Ground State phase diagram. Full line/diamonds: DFT ground-state energies, squares/dotted line: CE ground-state energies. $L1_2$ Ni_3Al is reproduced, yet the predicted heat of formation is far too low. $L1_0$ NiAl is no predicted ground-state.

calculated. The mean value of these k mean deviations

$$CVS^2 = \frac{1}{k\frac{N}{k}} \sum_{k} \sum_{\sigma \text{in test set}} \left[E_{DFT}(\sigma) - E_{CE}(\sigma)\right]^2 \qquad (3.2)$$

is denoted the k-fold Cross Validation Error (or Score, CVS). According to how many measuring points are in the test set, either 1 ore more, it is denoted *Leave One Out* (LOO) or *Leave Many Out* (LMO) -CVS. Note that particularly for large input sets it is not obligatory that all test sets contain the same number of elements; the CVS is indeed simply the mean of all mean test set prediction errors.

The CVS is a measure of the predictive power of the model equation fitted to *all* measuring points. It is hence a measure of prediction accuracy *without losing information* by excluding datapoints from the fit to use for testing.

Chapter 4

Results, Discussion and Outlook

Figure 4.5 shows the the deviations of the LCE predictions and the DFT calculations for ΔE_i^{eff} for the three test configurations (σ_6,σ_{10},σ_{13}). The error bars are the respective CVS. The smallest CVS correspond to a relative error of only 0.1% The majority of the LCEs reproduce the test set energies reasonably well. Among the LCEs with the smallest CVS, LCEs 51, 52, 53, 55, 56, 57, 58, 60 make the best predictions. The LECIs of nos. 56, 58 are shown in the figures below. Their validity, of course, is limited to the concentration range of the input set, $c_{Al} \approx 0.25$ [26, 30, 32].

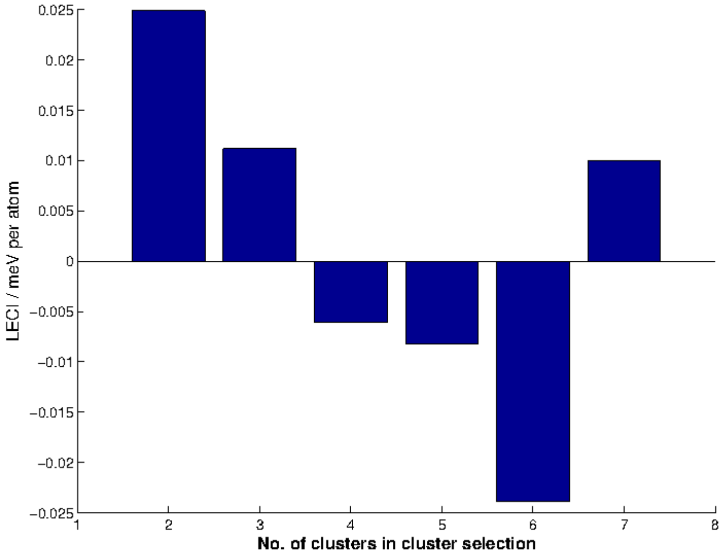

Figure 4.1: Absolute values of the LECIs of LCE no. 56, in meV/atom

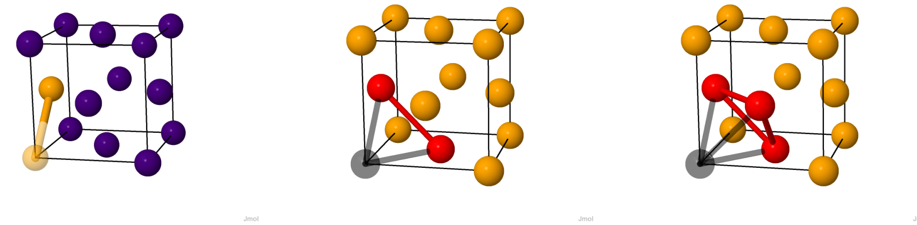

(a) Cluster no.(2) (b) Cluster no.(5) (c) Cluster no.(7)

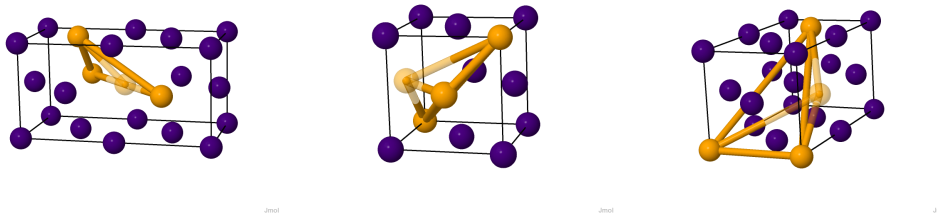

(d) Cluster no.(13) (e) Cluster no.(16) (f) Cluster no.(23)

Figure 4.2: The clusters of LCE no. 56

The dominant contribution is the null cluster, due to its large value of (-4.4) meV/atom not depicted in the figures. Its value hardly differs for all LCEs. We note that each LECI (Clusters 1,2,5,7,13) which is included in both LCEs has the same value for both calculations.

As mentioned in the previous chapter the simplified algorithm for the global binary CE, however, could not achieve a robust CE for the Ni-Al-system (cf. Phase diagram figure 3.2). The calculation of the ECIs should be improved by the implementation as MSCE and the use of the GA. Another possible reason are the input DFT calculations, due to the magnetic properties of the system and due to relaxation: particularly for $L1_0$ NiAl *full relaxation* might lead to a phase transformation to B_2 NiAl, which is the physical ground state [49]. Hence further effort is required for the full description of binary systems with dilute vacancies according to Eqn. 2.45

The description of the atomic jump profiles through LCE and CE within transition state theory [2], similar to the calculation of diffusion barriers in Ref. [43], remains a long-term aim.

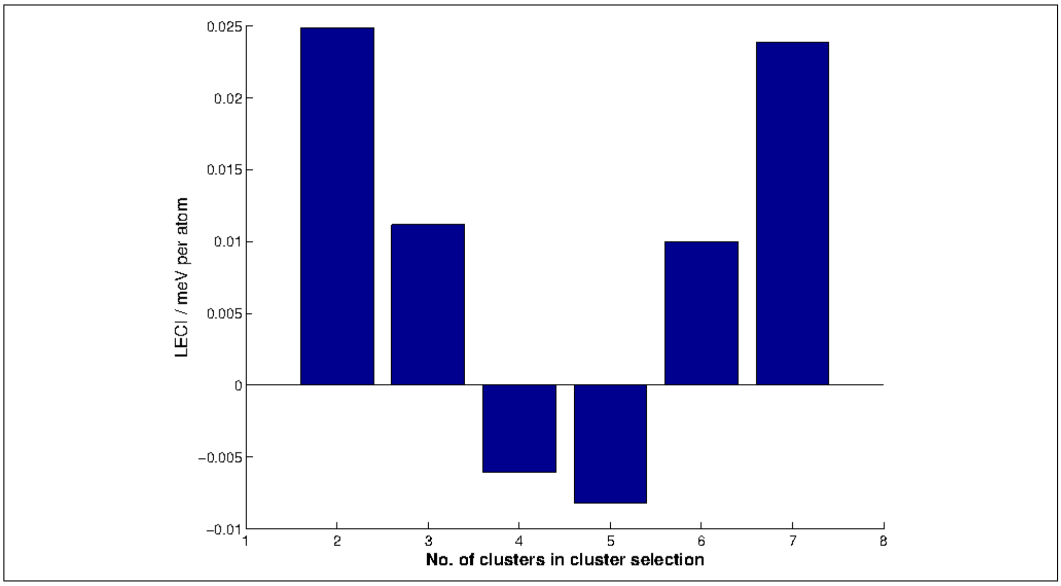

Figure 4.3: Absolute values of the LECIs of LCE no. 58, in meV/atom

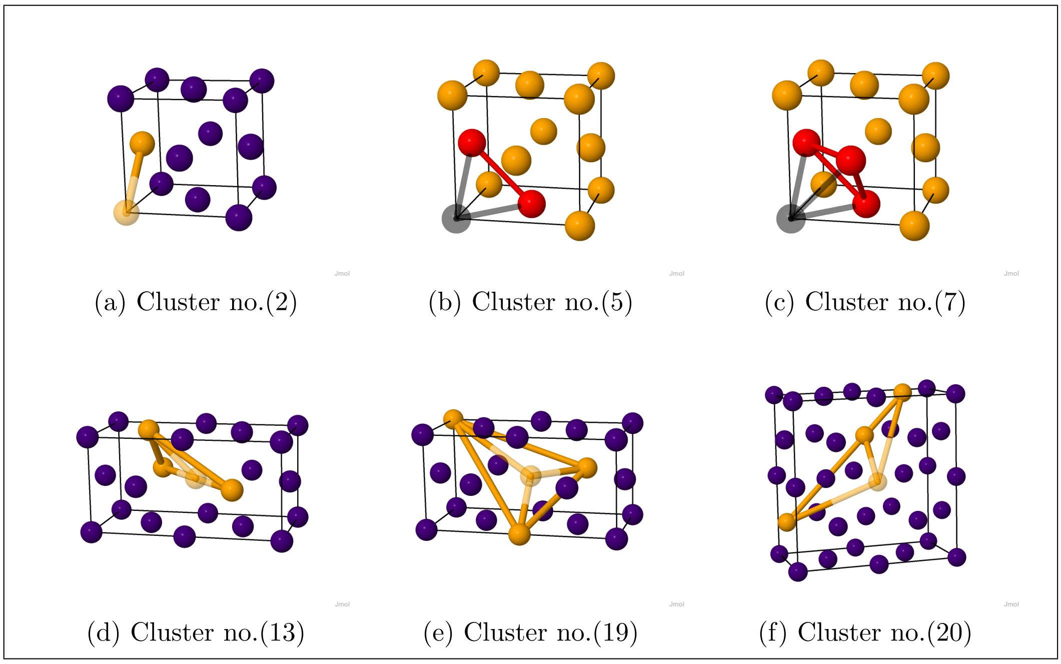
(a) Cluster no.(2)
(b) Cluster no.(5)
(c) Cluster no.(7)
(d) Cluster no.(13)
(e) Cluster no.(19)
(f) Cluster no.(20)

Figure 4.4: The clusters of LCE no. 58

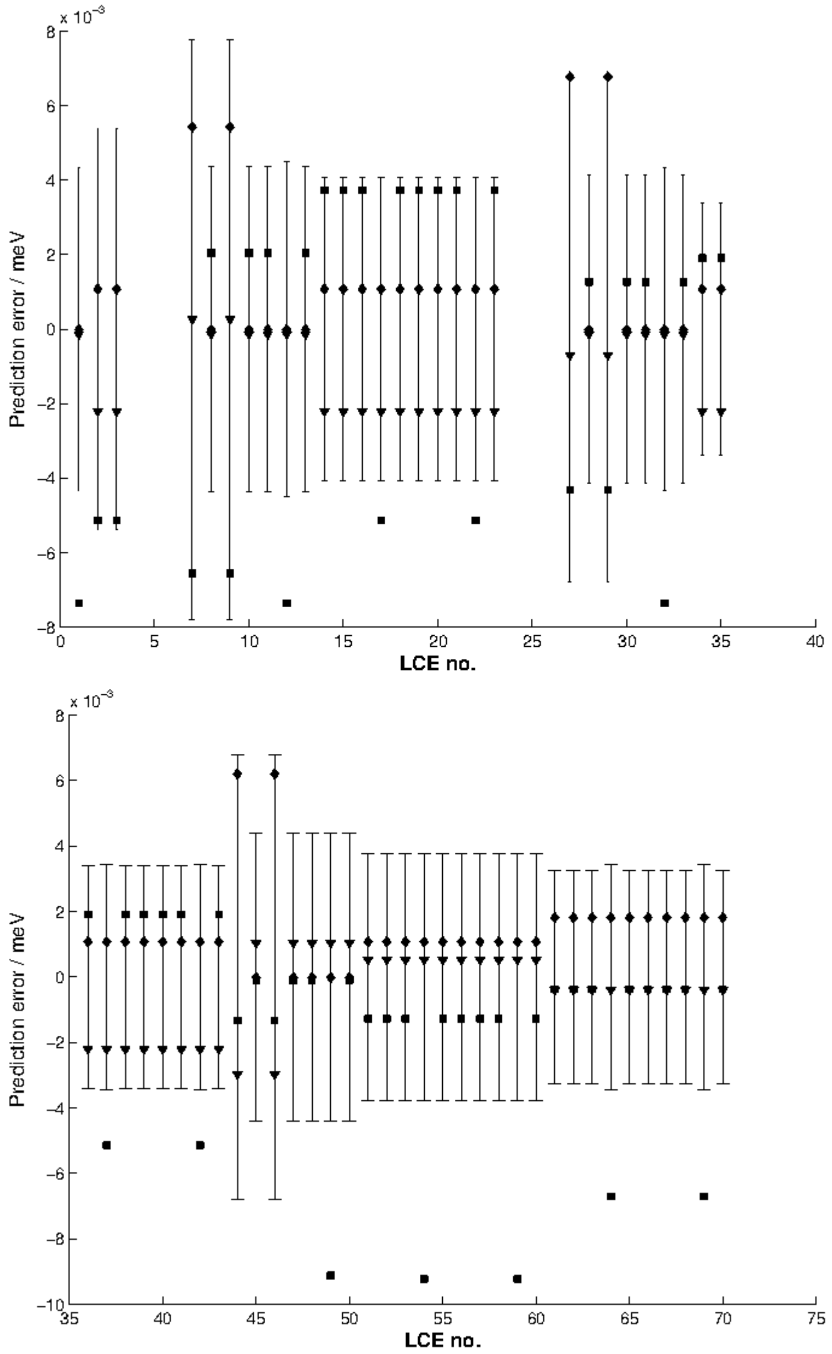

Figure 4.5: Absolute deviation of E_{CE} from E_{DFT} in meV/atom. Diamonds: Testconfiguration σ_6; Squares: Testconfiguration σ_{10}, Triangle: Testconfiguration σ_{13}. The x-axis denotes the number of the LCE (cluster selection). LCEs no. $3, 4, 5, 24, 25, 26$ are left out due to a very large deviation, see Appendix for full set.

Bibliography

[1] D. Caillard. Dislocations and mechanical properties. In W. Pfeiler, editor, *Alloy physics: a comprehensive reference*, chapter 6, pages 281–346. Wiley-VHC Verlag GmbH & Co KGaA, Weinheim, 2007.

[2] W. Püschl, H. Numakura, and W. Pfeiler. Point defects, atom jumps and diffusion. In W. Pfeiler, editor, *Alloy physics: a comprehensive reference*, chapter 5, pages 173–280. Wiley-VHC Verlag GmbH & Co KGaA, Weinheim, 2007.

[3] Q. Xu and A. Van der Ven. First-principles investigation of migration barriers and point defect complexes in B2–NiAl. *Intermetallics*, 17(5):319–329, May 2009.

[4] A. Van der Ven. *First Principles Investigation of Thermodynamic and Kinetic Properties of Lithium Transition Metal Oxides.* PhD thesis, Massachusetts Instutute of Technology, 2000.

[5] F Haider, R Kozubski, and T.A. Abinandanan. Simulation Techniques. In W. Pfeiler, editor, *Alloy physics: a comprehensive reference*, chapter 12, pages 653–706. Wiley-VHC Verlag GmbH & Co KGaA, Weinheim, 2007.

[6] N. W. Ashcroft and D. N. Mermin. *Festkörperphysik.* Oldenburg, 3 edition, 2007.

[7] P. Hohenberg and W. Kohn. Inhomogeneous Electron Gas. *Physical Review*, 136(3B):B864–B871, November 1964.

[8] W. Kohn and L. J. Sham. Self-Consistent Equations Including Exchange and Correlation Effects. *Physical Review*, 140(4A):A1133–A1138, November 1965.

[9] S Müller, W. Wolf, and R. Podloucky. Ab initio methods and applications. In W. Pfeiler, editor, *Alloy physics: a comprehensive refer-*

ence, chapter 11, pages 589–652. Wiley-VHC Verlag GmbH & Co KGaA, Weinheim, 2007.

[10] A. V. Ruban and I. A. Abrikosov. Configurational thermodynamics of alloys from first principles: effective cluster interactions. *Reports on Progress in Physics*, 71(4):046501, April 2008.

[11] J.M. Sanchez, F. Ducastelle, and D. Gratias. Generalized cluster description of multicomponent systems. *Physica A: Statistical Mechanics and its Applications*, 128(1-2):334–350, November 1984.

[12] C. Wolverton and D. de Fontaine. Cluster expansions of alloy energetics in ternary intermetallics. *Physical Review B*, 49(13):8627–8642, April 1994.

[13] A. Van der Ven and G. Ceder. Vacancies in ordered and disordered binary alloys treated with the cluster expansion. *Physical Review B*, 71(5):1–7, February 2005.

[14] D. Morgan, J. D Althoff, and D De Fontaine. Local Environment Effects in the Vibrational Properties of Disordered Alloys: an Embedded - Atom Method Study of Ni3AI and Cu3Au. *Journal of Phase Equilibria*, 19(6):559–567, 1998.

[15] D. Morgan, A. Van De Walle, G. Ceder, J.D. Althoff, and D. DeFontaine. Vibrational thermodynamics: coupling of chemical order and size effects. *Modelling and Simulation in Materials Science and Engineering*, 8(3):295–309, May 2000.

[16] S. Müller. Bulk and surface ordering phenomena in binary metal alloys. *Journal of Physics: Condensed Matter*, 15(34):R1429–R1500, 2003.

[17] V. Blum, G. Hart, M. Walorski, and A. Zunger. Using genetic algorithms to map first-principles results to model Hamiltonians: Application to the generalized Ising model for alloys. *Physical Review B*, 72(16):1–13, October 2005.

[18] A. van de Walle, M. Asta, and G. Ceder. The alloy theoretic automated toolkit: A user guide. *Calphad*, 26(4):539–553, December 2002.

[19] D. Lerch, O. Wieckhorst, G. L. W. Hart, R. W. Forcade, and S. Müller. UNCLE: a code for constructing cluster expansions for arbitrary lattices with minimal user-input. *Modelling and Simulation in Materials Science and Engineering*, 17(5):055003, September 2009.

[20] R. Kikuchi. A Theory of Cooperative Phenomena. *Physical Review*, 81(6):988–1003, 1951.

[21] D. De Fontaine. Configurational Thermodynamics of Solid Solutions. *Solid State Physics*, 34:73, 1979.

[22] J.M. Sanchez and D. De Fontaine. Theoretical Prediction of Ordered Superstructures in Metallic Alloys. *Structure and Bonding in Crystals*, 2:117, 1981.

[23] J.W.D. Connolly and A.R. Williams. Density-functional theory applied to phase transformations in transition-metal alloys. *Physical Review B*, 27(8):5169, 1983.

[24] Z. Lu, S.-H. Wei, A. Zunger, S. Frota-Pessoa, and L. Ferreira. First-principles statistical mechanics of structural stability of intermetallic compounds. *Physical Review B*, 44(2):512–544, July 1991.

[25] D. De Fontaine. Cluster Approach to Order-Disorder Transformations in Alloys. *Solid State Physics*, 47:33–176, 1994.

[26] A. Zunger. First-principles statistical mechanics of semiconductor alloys and intermetallic compounds. *NATO ASI SERIES B PHYSICS*, 319:361–419, 1994.

[27] T. Mohri. Statistical thermodynamics and model calculations. In W. Pfeiler, editor, *Alloy physics: a comprehensive reference*, chapter 10, pages 525–588. Wiley-VHC Verlag GmbH & Co KGaA, Weinheim, 2007.

[28] Y. Grin, U. Scharz, and W Steurer. Crystal structure and chemical bonding. In W. Pfeiler, editor, *Alloy physics: a comprehensive reference*, chapter 2, pages 19–62. Wiley-VHC Verlag GmbH & Co KGaA, Weinheim, 2007.

[29] Y. Chen, T. Atago, and T. Mohri. First-principles study for ordering and phase separation in the Fe-Pd system. *Journal of Physics: Condensed Matter*, 14(8):1903–1913, March 2002.

[30] M. Asta, C. Wolverton, D. De Fontaine, and H. Dreyssé. Effective cluster interactions from cluster-variation formalism. I. *Physical Review B*, 44(10):4907–4913, 1991.

[31] N. Zarkevich and D. Johnson. Reliable First-Principles Alloy Thermodynamics via Truncated Cluster Expansions. *Physical Review Letters*, 92(25):255702–1–4, June 2004.

[32] M. Asta, C. Wolverton, D. De Fontaine, and H. Dreyssé. Effective cluster interactions from cluster-variation formalism. II. *Physical Review B*, 44(10):4914–4924, 1991.

[33] A. Walle and G. Ceder. Automating first-principles phase diagram calculations. *Journal of Phase Equilibria*, 23(4):348–359, August 2002.

[34] G. Hart, V. Blum, M. Walorski, and A. Zunger. Evolutionary approach for determining first-principles hamiltonians. *Nature materials*, 4(5):391–4, May 2005.

[35] C. Lang and N. Pucker. *Mathematische Me.* Spektrum Akademischer Verlag (Spektrum Hochschultaschenbuch), Heidelberg; Berlin, 1998.

[36] S. Arlot and A. Celisse. A survey of cross-validation procedures for model selection. *Statistics Surveys*, 4:40–79, 2010.

[37] S. Barabash, V. Blum, S. Müller, and A. Zunger. Prediction of unusual stable ordered structures of Au-Pd alloys via a first-principles cluster expansion. *Physical Review B*, 74(3):035108, July 2006.

[38] D.B. Laks, L.G. Ferreira, S. Froyen, and A. Zunger. Efficient cluster expansion for substitutional systems. *Physical Review B*, 46(19):12587–12605, 1992.

[39] C. Wolverton, G. Ceder, D. De Fontaine, and H. Dreyssé. Ab initio determination of structural stability in fcc-based transition-metal alloys. *Physical Review B*, 48(2):726–747, 1993.

[40] A. Zunger, LG Wang, G. . Hart, and M. Sanati. Obtaining Ising-like expansions for binary alloys from first principles. *Modelling and Simulation in Materials Science and Engineering*, 10:685–706, 2002.

[41] Q. Xu. *First-principles investigantion of thermodynamic and kinetic properties in Ti-H System and B2-NiAl compound: Phase stability, point defect complexes and diffusion.* PhD thesis, The University of Michigan, 2009.

[42] A. Van der Ven, M. K Aydinol, G. Ceder, G. Kresse, and J. Hafner. First-principles investigation of phase stability in Li. *Physical Review B*, 58(6):2975–2987, 1998.

[43] A. Van der Ven, G. Ceder, M. Asta, and P. Tepesch. First-principles theory of ionic diffusion with nondilute carriers. *Physical Review B*, 64(18):1–17, October 2001.

[44] G. Kresse and J. Hafner. Ab initio molecular dynamics for liquid metals. *Physical Review B*, 47(1):558–561, January 1993.

[45] G. Kresse and J. Furthmüller. Efficient iterative schemes for ab initio total-energy calculations using a plane-wave basis set. *Physical Review B*, 54(16):11169–11186, October 1996.

[46] G. Kresse and D. Joubert. From ultrasoft pseudopotentials to the projector augmented-wave method. *Physical Review B*, 59(3):1758–1775, January 1999.

[47] G. Kresse and J. Furthmüller. Efficiency of ab-initio total energy calculations for metals and semiconductors using a plane-wave basis set. *Computational Materials Science*, 6(1):15–50, July 1996.

[48] G Kresse and J Hafner. Norm-conserving and ultrasoft pseudopotentials for first-row and transition elements. *Journal of Physics: Condensed Matter*, 6(40):8245–8257, October 1994.

[49] M. Leitner. Unpublished.

[50] R. Freund and R. Hoppe. *Stoer/Bulirsch: Numerische Mathematik 1*. Springer Berlin Heidelberg, Berlin, Heidelberg, 10 edition, 2007.

[51] A. Van der Ven and G. Ceder. First Principles Calculation of the Interdiffusion Coefficient in Binary Alloys. *Physical Review Letters*, 94(4), February 2005.

Appendix A

Supplements to the LCE Results and Documentation

Table A.1: The configurations for the input set and test set for the LCE I

Defect Configurations of $L1_2$ $\mathrm{Ni_3Al}$		
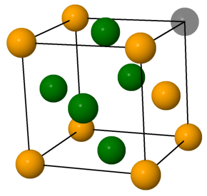	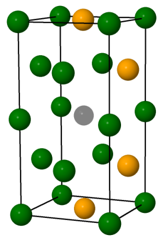	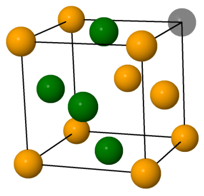
Config.no. 1	Config.no. 2	Config.no. 3
$(3,2,2)$ Al	$(3,2,2)$ Al $(3,2,4)$ Al	$(3,2,2)$ Al $(2,3,2)$ Al
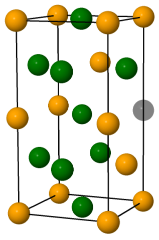	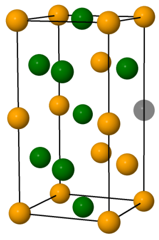	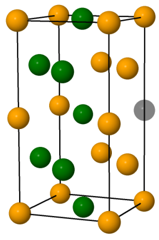
Config.no. 4	Config.no. 5	Config.no. 6
$(3,2,2)$ Al $(2,3,4)$ Al	$(3,2,2)$ Al $(2,3,4)$ Al $(2,3,2)$ Al	$(3,2,4)$ Al $(3,2,2)$ Al $(2,3,4)$ Al $(2,3,2)$ Al
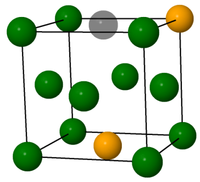	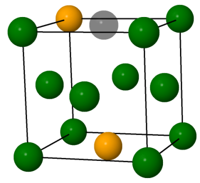	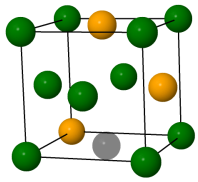
Config.no. 7	Config.no. 8	Config.no. 9
$(4,4,3)$ Al	$(2,4,3)$ Al $(2,2,3)$ Al	$(4,3,4)$ Al $(2,4,3)$ Al
$a_{fcc} = 2$. Ni:green, Al:yellow. The shaded atom is a vacancy at the Al-sublattice at $(3,3,3)$.		

Table A.2: The configurations for the input set and test set for the LCE II

Defect Configurations of $D0_{22}$ Ni_3Al		
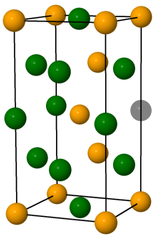	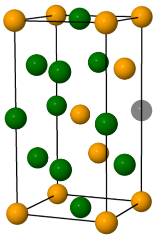	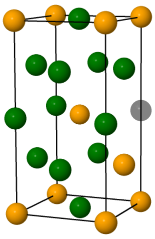
Config.no. 10	Config.no. 11	Config.no. 12
$(2,3,2)$ Ni $(2,3,4)$ Ni	$(3,2,4)$ Al $(2,3,2)$ Al	$(3,2,2)$ Al $(2,3,2)$ Ni
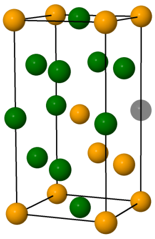	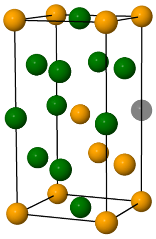	
Config.no. 13	Config.no. 14	
$(3,2,2)$ Al $(2,3,2)$ Al	$(3,2,2)$ Al $(3,2,4)$ Al	
$a_{fcc} = 2$. Ni:green, Al:yellow. The shaded atom is a vacancy at the Ni-sublattice at $(3,3,3)$.		

All pictures were created using
Jmol: an open-source Java viewer for chemical structures in 3D
http://www.jmol.org/

Table A.3: List of Selected Clusters of each LCE

LCE no.	Cluster Selection	LCE no.	Cluster Selection
1	1, 2, 5, 7, 11, 12, 14	2	1, 2, 5, 7, 11, 12, 14
3	1, 2, 5, 7, 11, 12, 19	4	1, 2, 5, 7, 11, 12, 19
5	1, 2, 5, 7, 11, 13, 16	6	1, 2, 5, 7, 11, 13, 16
7	1, 2, 5, 7, 11, 14, 16	8	1, 2, 5, 7, 11, 14, 16
9	1, 2, 5, 7, 11, 14, 19	10	1, 2, 5, 7, 11, 14, 19
11	1, 2, 5, 7, 11, 14, 21	12	1, 2, 5, 7, 11, 14, 21
13	1, 2, 5, 7, 11, 14, 23	14	1, 2, 5, 7, 11, 14, 23
15	1, 2, 5, 7, 11, 16, 20	16	1, 2, 5, 7, 11, 16, 20
17	1, 2, 5, 7, 11, 16, 22	18	1, 2, 5, 7, 11, 16, 22
19	1, 2, 5, 7, 11, 17, 19	20	1, 2, 5, 7, 11, 17, 19
21	1, 2, 5, 7, 11, 19, 21	22	1, 2, 5, 7, 11, 19, 21
23	1, 2, 5, 7, 11, 19, 23	24	1, 2, 5, 7, 11, 19, 23
25	1, 2, 5, 7, 12, 13, 16	26	1, 2, 5, 7, 12, 13, 16
27	1, 2, 5, 7, 12, 14, 16	28	1, 2, 5, 7, 12, 14, 16
29	1, 2, 5, 7, 12, 14, 19	30	1, 2, 5, 7, 12, 14, 19
31	1, 2, 5, 7, 12, 14, 21	32	1, 2, 5, 7, 12, 14, 21
33	1, 2, 5, 7, 12, 14, 23	34	1, 2, 5, 7, 12, 14, 23
35	1, 2, 5, 7, 12, 16, 20	36	1, 2, 5, 7, 12, 16, 20
37	1, 2, 5, 7, 12, 16, 22	38	1, 2, 5, 7, 12, 16, 22
39	1, 2, 5, 7, 12, 17, 19	40	1, 2, 5, 7, 12, 17, 19
41	1, 2, 5, 7, 12, 19, 21	42	1, 2, 5, 7, 12, 19, 21
43	1, 2, 5, 7, 12, 19, 23	44	1, 2, 5, 7, 12, 19, 23
45	1, 2, 5, 7, 13, 14, 17	46	1, 2, 5, 7, 13, 14, 17
47	1, 2, 5, 7, 13, 14, 20	48	1, 2, 5, 7, 13, 14, 20
49	1, 2, 5, 7, 13, 14, 22	50	1, 2, 5, 7, 13, 14, 22
51	1, 2, 5, 7, 13, 16, 17	52	1, 2, 5, 7, 13, 16, 17
53	1, 2, 5, 7, 13, 16, 21	54	1, 2, 5, 7, 13, 16, 21
55	1, 2, 5, 7, 13, 16, 23	56	1, 2, 5, 7, 13, 16, 23
57	1, 2, 5, 7, 13, 19, 20	58	1, 2, 5, 7, 13, 19, 20
59	1, 2, 5, 7, 13, 19, 22	60	1, 2, 5, 7, 13, 19, 22
61	1, 2, 5, 7, 14, 16, 17	62	1, 2, 5, 7, 14, 16, 17
63	1, 2, 5, 7, 14, 16, 21	64	1, 2, 5, 7, 14, 16, 21
65	1, 2, 5, 7, 14, 16, 23	66	1, 2, 5, 7, 14, 16, 23
67	1, 2, 5, 7, 14, 19, 20	68	1, 2, 5, 7, 14, 19, 20
69	1, 2, 5, 7, 14, 19, 22	70	1, 2, 5, 7, 14, 19, 22

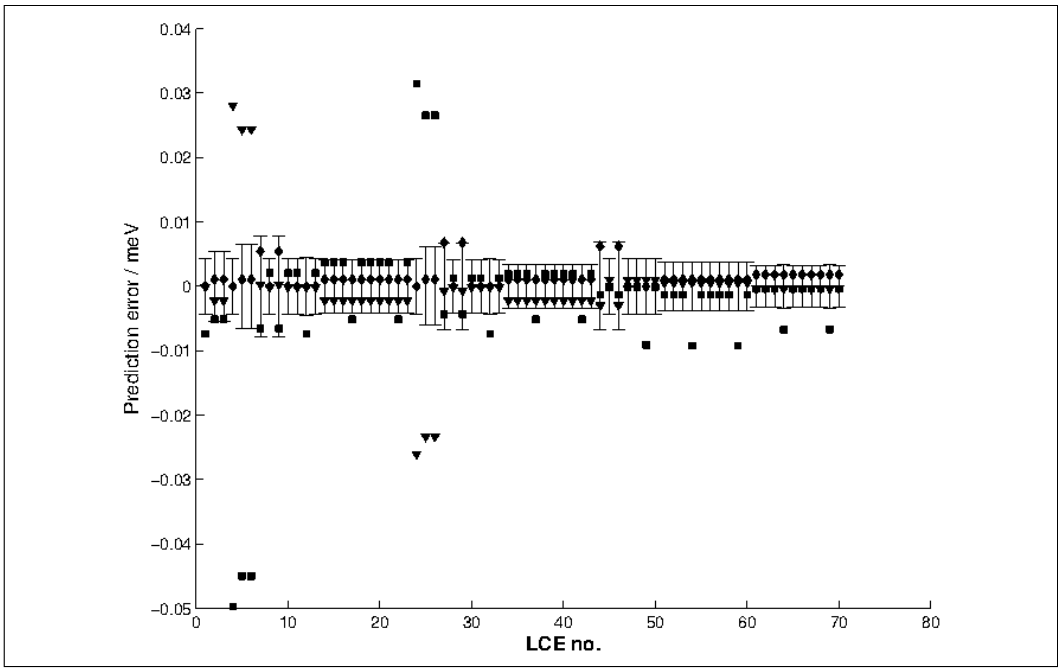

Figure A.1: Absolute deviation of E_{CE} from E_{DFT}. Diamonds: Testconfiguration 1; Squares: Testconfiguration 2, Triangle: Testconfiguration 3

Appendix B

Curriculum Vitae

Barbara Knöbl

Personal

Date of birth: September 8, 1985

Birthplace: Oberwart, Austria

Citizenship: Austrian

Education

Student of Physics
University of Vienna, Austria
October 2004 - present
With a concentration on Solid State Physics

Semester abroad (ERASMUS)
Technische Universität Berlin, Germany

High school with focus on languages
Bundesgymnasium 21, Franklinstraße 26
September 1996 - June 2004
Reifeprüfung with distinction

Last updated: August 28, 2012